

Fluid dynamics and dynamo action in planetary cores

Hagay Amit

Laboratoire de Planétologie et Géosciences, CNRS, Nantes
Université

October 2022



Outline

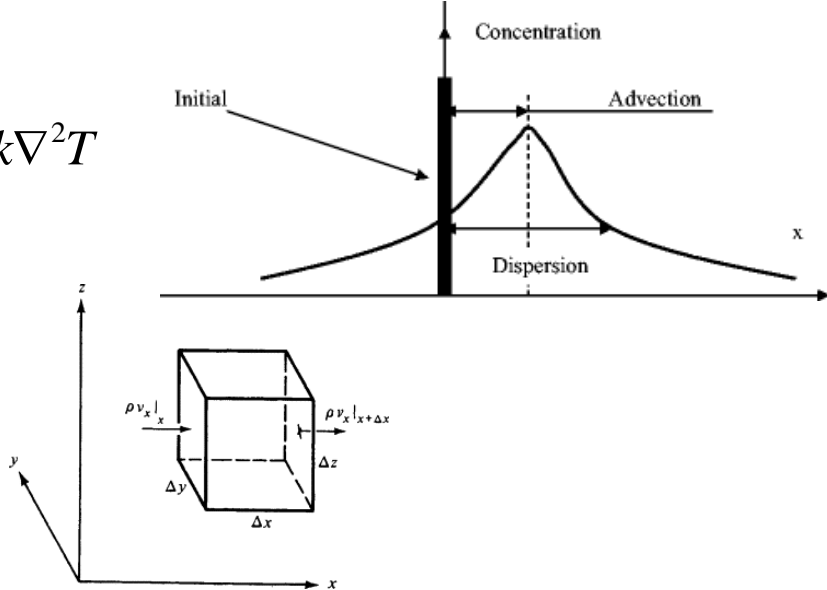
1. Fundamentals of fluid dynamics - governing equations, non-dimensional numbers, difference between mantle and core dynamics
2. Thermo-chemical core convection - Convection types and boundary conditions for core dynamics
3. Rotational effects - geostrophy, Taylor-Proudman constraint, Ekman boundary layer, tangent cylinder
4. Dynamo theory - Maxwell's equations, magnetic induction equation, magnetostrophy, frozen-flux, necessary ingredients for a dynamo, generation mechanisms
5. Observations - Seismology, geomagnetic/archeomagnetic/paleomagnetic field models, reversals, geodesy, magnetic fields of other planets
6. Core flow inversions - assumptions, results, problems, progress
7. Numerical dynamos - successes, problems, progress

1. Fundamentals of fluid dynamics - governing equations

Navier-Stokes (conservation of momentum): $\frac{\partial \vec{u}}{\partial t} + \vec{u} \cdot \nabla \vec{u} - \nu \nabla^2 \vec{u} + 2\Omega \hat{z} \times \vec{u} + \frac{1}{\rho} \nabla P = \alpha g T \hat{r}$

Heat (conservation of energy): $\frac{\partial T}{\partial t} + \vec{u} \cdot \nabla T = k \nabla^2 T$

Continuity (conservation of mass): $\nabla \cdot \vec{u} = 0$



1. Fundamentals of fluid dynamics- non-dimensional form

Navier-Stokes (conservation of momentum): $E\left(\frac{\partial \vec{u}}{\partial t} + \vec{u} \cdot \nabla \vec{u} - \nabla^2 \vec{u}\right) + 2\hat{z} \times \vec{u} + \nabla P = Ra \frac{\vec{r}}{R} T$

Heat (conservation of energy): $\frac{\partial T}{\partial t} + \vec{u} \cdot \nabla T = \frac{1}{Pr} \nabla^2 T$

Continuity (conservation of mass): $\nabla \cdot \vec{u} = 0$

Input:

Heat flux Rayleigh $Ra = \frac{\alpha g_0 q_0 D^4}{\nu k \kappa}$

Ekman $E = \frac{\nu}{\Omega D^2}$

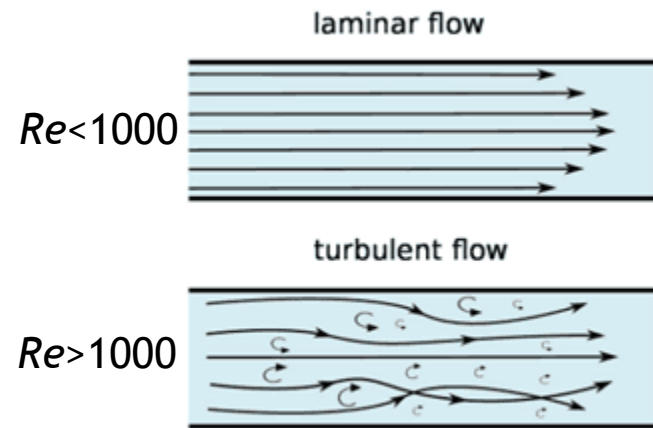
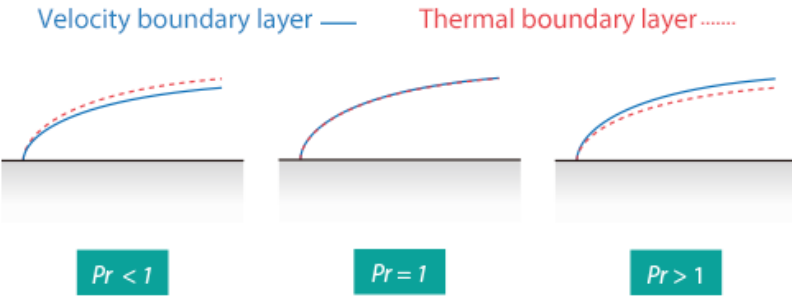
Prandtl $Pr = \frac{\nu}{\kappa}$

Some output:

Reynolds $Re = \frac{UD}{\nu}$

Rossby $Ro = \frac{U}{\Omega D}$

1. Fundamentals of fluid dynamics - non-dimensional form



Input:

$$\text{Heat flux Rayleigh} \quad Ra = \frac{\alpha g_0 q_0 D^4}{\nu k \kappa}$$

$$\text{Ekman} \quad E = \frac{\nu}{\Omega D^2}$$

$$\text{Prandtl} \quad Pr = \frac{\nu}{\kappa}$$

Some output:

$$\text{Reynolds} \quad Re = \frac{UD}{\nu}$$

$$\text{Rossby} \quad Ro = \frac{U}{\Omega D}$$

1. Difference between mantle and core dynamics

| Force/quantity | Mantle | Core |
|---------------------|--|---|
| Inertia (Re) | Small, no inertia/turbulence | Large, strong inertia/turbulence |
| Convection (Ra) | Larger than critical value, convecting | Larger than critical value, convecting |
| Viscosity | Temperature-dependent, complicated | Fluid property, well mixed conditions, constant |
| Rotation (E) | Large, creeping flow | Small, inviscid flow, strong rotation effects |
| Rotation (Ro) | Not relevant | Small, strong rotation effects |

Summary mantle: Creeping flow, gravity driven (perpendicular to isobars), no turbulence, no rotation effects, insulating.

Summary core: Inviscid flow, parallel to isobars (**geostrophy**), turbulent, strong rotation effects, electrically conducting.

2. Thermo-chemical core convection - convection types

Heat and light elements transport equations:

$$\frac{\partial T}{\partial t} + \vec{u} \cdot \nabla T = k_T \nabla^2 T + \varepsilon_T$$

$$\frac{\partial \chi}{\partial t} + \vec{u} \cdot \nabla \chi = k_\chi \nabla^2 \chi + \varepsilon_\chi$$

Thermal sources - secular cooling through CMB, radioactivity.

Chemical sources - light elements release at ICB.

Assuming same diffusivities (which is wrong!) gives a transport equation for the co-density $C = \alpha T + \beta \chi$:

$$\frac{\partial C}{\partial t} + \vec{u} \cdot \nabla C = k \nabla^2 C + \varepsilon$$

Distinctive diffusivities - double-diffusive convection (Bouffard et al., 2017).

2. Thermo-chemical core convection - boundary conditions

CMB:

Lateral thermal anomalies on mantle side ~100 K - mantle sees CMB as an isotherm.

Lateral thermal anomalies on core side ~1 mK, and mantle varies on much longer timescales - core sees CMB as a **fixed** (though heterogeneous) **heat flux**:

$$q_{CMB} = -K \frac{\partial T}{\partial r} = -K \frac{T_m - T_c}{\delta r} \approx -K \frac{T_m}{\delta r}$$

No mass exchange across the CMB:

$$\frac{\partial \chi}{\partial r} \Big|_{CMB} = 0$$

$$\frac{\partial C}{\partial r} \Big|_{CMB} \propto \frac{\partial T}{\partial r} \Big|_{CMB}$$

ICB:

Inner- core freezing releases **light elements and latent heat**.

Thermal convection - no IC growth, $\frac{\partial C}{\partial r} \Big|_{ICB} = 0$.

Chemical convection - prescribed $\frac{\partial C}{\partial r} \Big|_{ICB}$ corresponds to IC growth rate.

Volumetric **sources** balance heat loss from CMB in **thermal convection**; Volumetric **sinks** balance buoyancy input from light elements release in **chemical convection**.

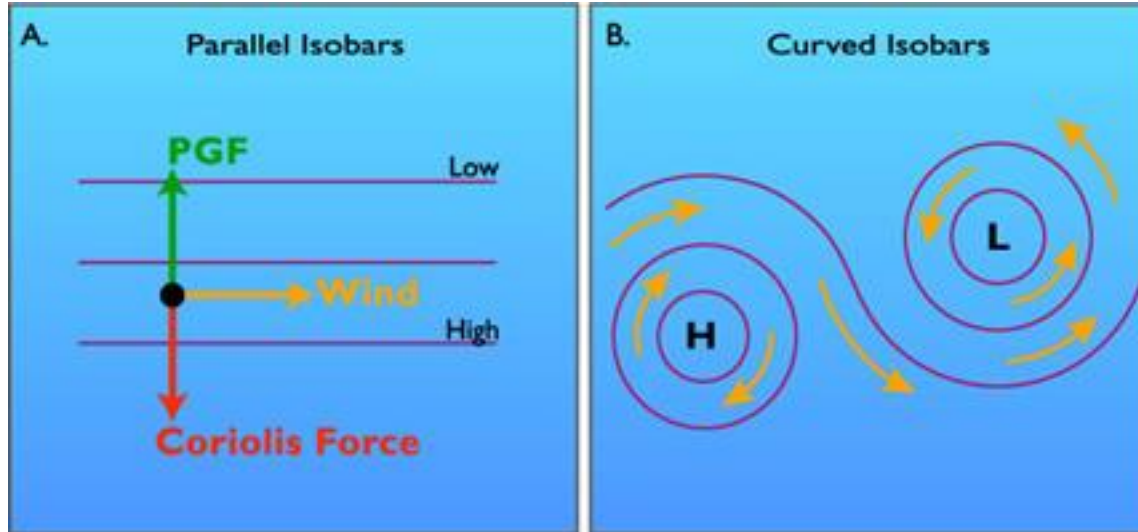
3. Rotational effects - geostrophy

Large E (mantle): Flow perpendicular to isobars ‘like a rolling stone’.



Small E and Ro (atmosphere, oceans, core): Geostrophic flow parallel to isobars:

$$2\Omega \hat{z} \times \vec{u} \approx -\frac{1}{\rho} \nabla P$$



Coriolis force deflects motions to the right (left) in NH (SH). In NH, downwelling (upwelling) in cyclones (anti-cyclones) correlates with anti-clockwise (clockwise) flow.

3. Rotational effects - columnar flow

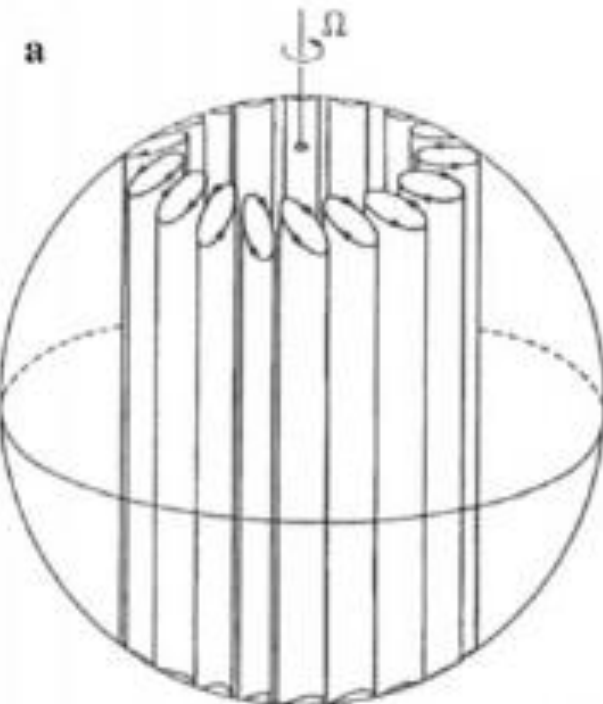
Under the Taylor-Proudman constraint the flow is invariant in the direction of the rotation axis:

$$\nabla \times \left[2\Omega \hat{z} \times \vec{u} \approx -\frac{1}{\rho} \nabla P \right] \Rightarrow \frac{\partial \vec{u}}{\partial z} = 0$$

According to quasi-geostrophy (QG) theory core flow is dominated by fluid columns aligned with the rotation axis that intercept the CMB at high-latitudes (Busse, 1975).

QG properties:

- Equatorial symmetry.
- CMB flow can be projected to the core volume.



3. Rotational effects - thermal wind

Keep the buoyancy term in the vorticity equation:

$$-2\Omega \frac{\partial \vec{u}}{\partial z} = \alpha g \nabla \times \hat{T r}$$

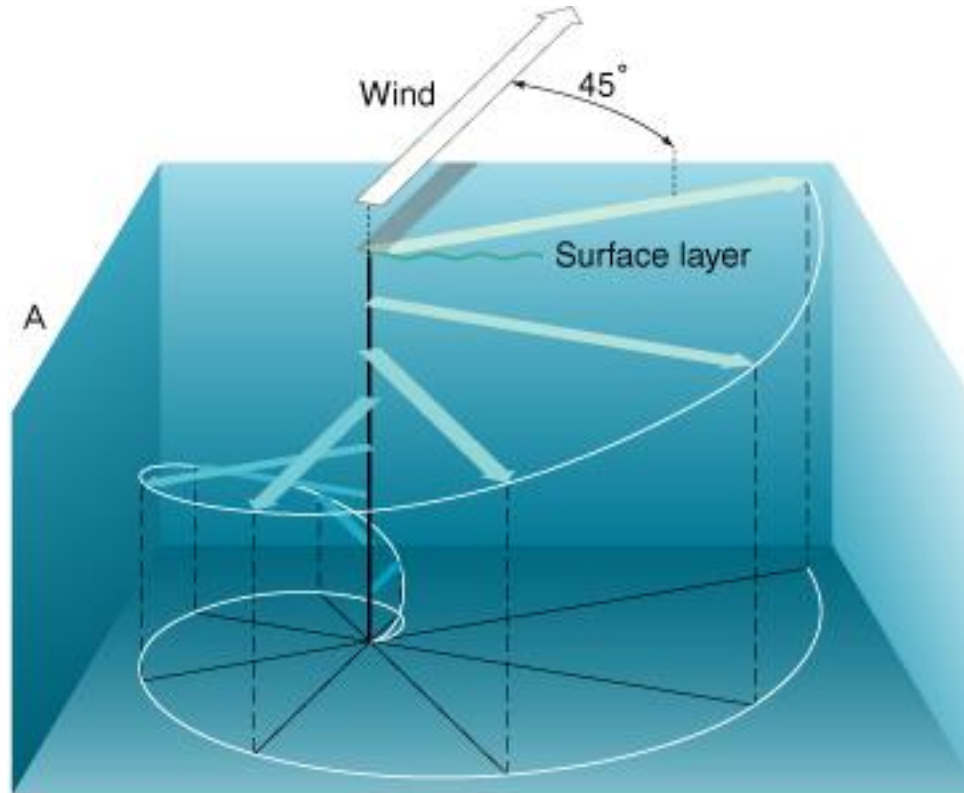
Horizontal components relate **vertical shear** of the flow to **horizontal gradient of the buoyancy**:

$$\frac{\partial u_\phi}{\partial z} = \frac{\alpha g}{2\Omega r} \frac{\partial T}{\partial \theta}$$

$$\frac{\partial u_\theta}{\partial z} = -\frac{\alpha g}{2\Omega r} \frac{1}{\sin \theta} \frac{\partial T}{\partial \phi}$$

3. Rotational effects - Ekman boundary layer

The **boundary layer flow** in a rapidly rotating system falls in magnitude (as in any viscous boundary layer) but also rotates due to the Coriolis force.

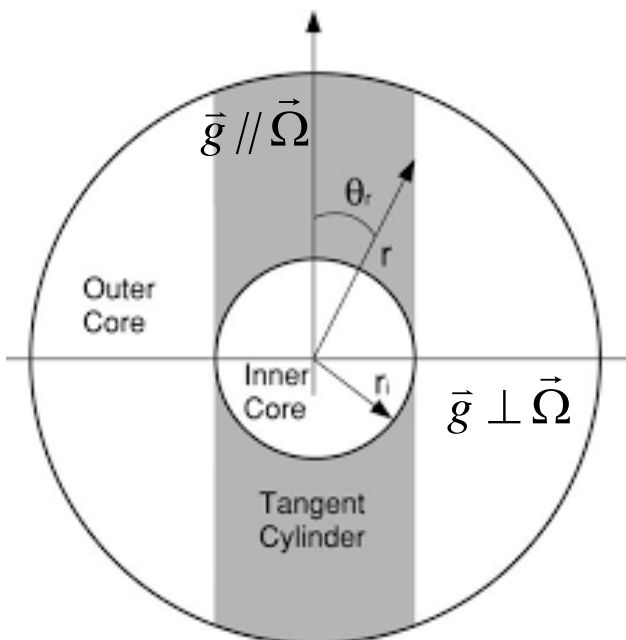


For Earth's core:

$$v = 1 \text{e-}6 \text{ m}^2/\text{s}, \Omega = 1 \text{e-}4 \text{ 1/s}, D = 1 \text{e}6 \text{ m}, E = 1 \text{e-}14, h_{ek} = \sqrt{ED} = 10 \text{ cm}$$

3. Rotational effects - tangent cylinder

Tangent cylinder latitude is correlated with intense magnetic flux patches on the CMB.

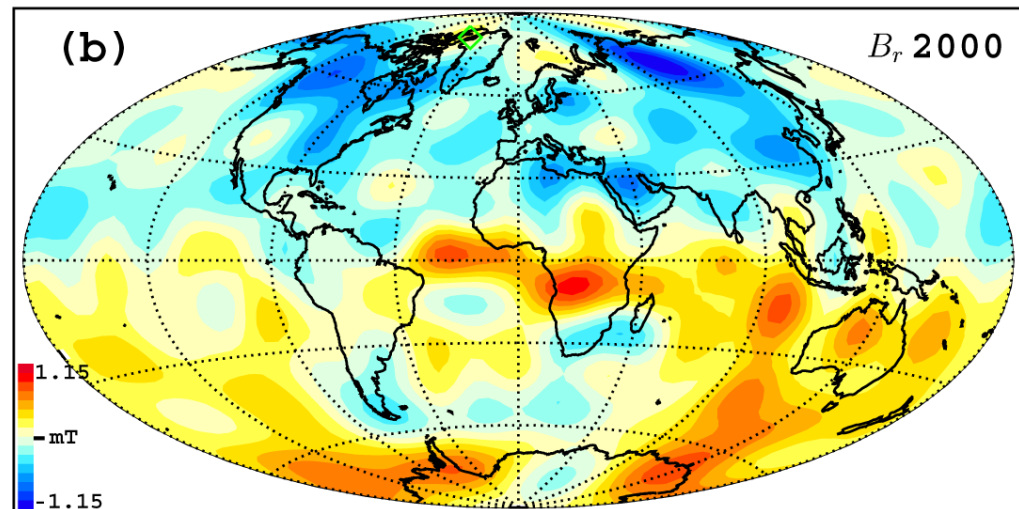
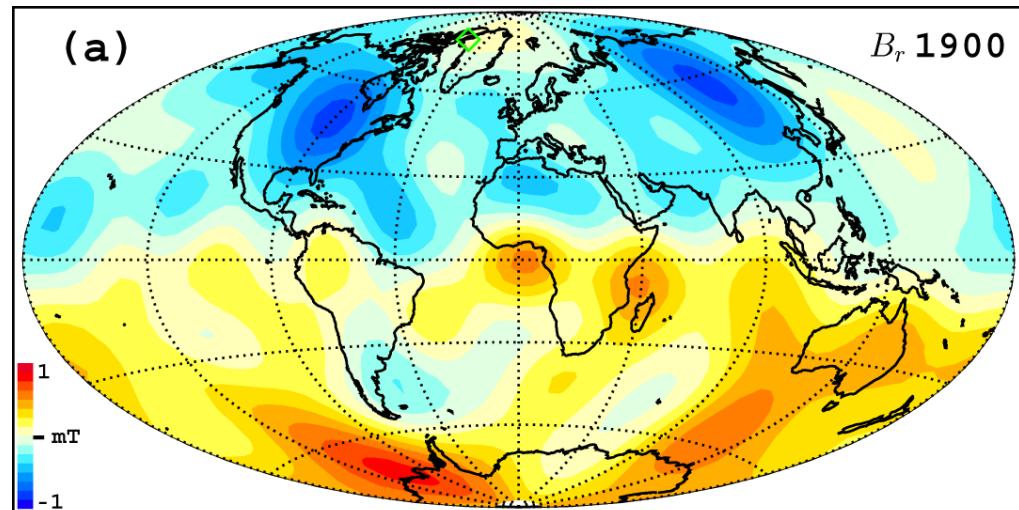


For Earth's core:

$$\sin(\theta_{tc}) = \frac{r_i}{r_o} = 0.35 \Rightarrow \theta_{tc} \approx 20^\circ$$

Tangent cylinder features:

- Flow barrier - convergence and intense patches on CMB.
- Separates dynamical regimes
 - outside **columnar flow**, inside **thermal wind**.



4. Dynamo theory - Maxwell's equations

Core fluid is electrically-conductive, must satisfy Maxwell's equations:

1. Gauss's law: Electrical field flux through a closed surface equals total electrical charge in volume. $\nabla \cdot \vec{E} = \frac{1}{\epsilon_0} \rho_e$
2. Faraday's law: Time-dependent magnetic field induces electrical field. $\nabla \times \vec{E} = -\frac{\partial \vec{B}}{\partial t}$
3. No magnetic monopoles: $\nabla \cdot \vec{B} = 0$
4. Ampére's law: Electrical current induces magnetic field lines around it. $\nabla \times \vec{B} = \mu_0 \vec{J}$
5. Ohm's law: Electromagnetic force. $\vec{J} = \sigma(\vec{E} + \vec{u} \times \vec{B})$

Three equations (2, 4, 5) with 4 variables (Electrical field, magnetic field, electrical current, velocity) - reduce to one magnetic field transport equation with 2 variables, the **magnetic induction equation**:

$$\frac{\partial \vec{B}}{\partial t} = \nabla \times (\vec{u} \times \vec{B}) + \lambda \nabla^2 \vec{B}$$

Field changes are due to advection and diffusion - analog to heat transport.

4. Dynamo theory - MHD equations

Full set of non-dimensional MHD equations for an electrically-conductive, Boussinesq, incompressible fluid in a rotating convecting spherical shell (e.g. Olson and Christensen, 2002):

Navier-Stokes (conservation of momentum):

$$E \left(\frac{\partial \vec{u}}{\partial t} + \vec{u} \cdot \nabla \vec{u} - \nabla^2 \vec{u} \right) + 2\hat{z} \times \vec{u} + \nabla P = Ra \frac{\vec{r}}{R} T + \frac{1}{Pm} (\nabla \times \vec{B}) \times \vec{B}$$

Induction (Maxwell's equations of electromagnetism):

$$\frac{\partial \vec{B}}{\partial t} = \nabla \times (\vec{u} \times \vec{B}) + \frac{1}{Pm} \nabla^2 \vec{B}$$

Heat (conservation of energy):

$$\frac{\partial T}{\partial t} + \vec{u} \cdot \nabla T = \frac{1}{Pr} \nabla^2 T$$

Continuity (conservation of mass):

$$\nabla \cdot \vec{u} = 0$$

No magnetic monopoles:

$$\nabla \cdot \vec{B} = 0$$

Heat flux Rayleigh $Ra = \frac{\alpha g_0 q_0 D^4}{\nu k \kappa}$

Ekman $E = \frac{\nu}{\Omega D^2}$

Prandtl $Pr = \frac{\nu}{\kappa}$

magnetic Prandtl $Pm = \frac{\nu}{\lambda}$

4. Dynamo theory - more non-dimensional numbers

Magnetostrophic force balance:

$$2\Omega \hat{z} \times \vec{u} + \frac{1}{\rho} \nabla P \approx \frac{1}{\rho \mu_0} (\nabla \times \vec{B}) \times \vec{B}$$

Elsasser number measures field strength:

$\Lambda > 1$ is termed ‘strong field’.

Dynamic Elsasser number better captures strength of Lorentz force
(Soderlund et al., 2012):

$$\Lambda_d = \frac{B^2}{\rho \mu \Omega U D}$$

Magnetic Reynolds number measures field advection vs. diffusion:

$$Rm = \frac{UD}{\lambda}$$

For Earth’s core: $U=5e-4$ m/s (for a review see Holme, 2015), $D=2e6$ m, $\lambda=1$ m²/s, $Rm=1000 \gg 1$. Consequences:

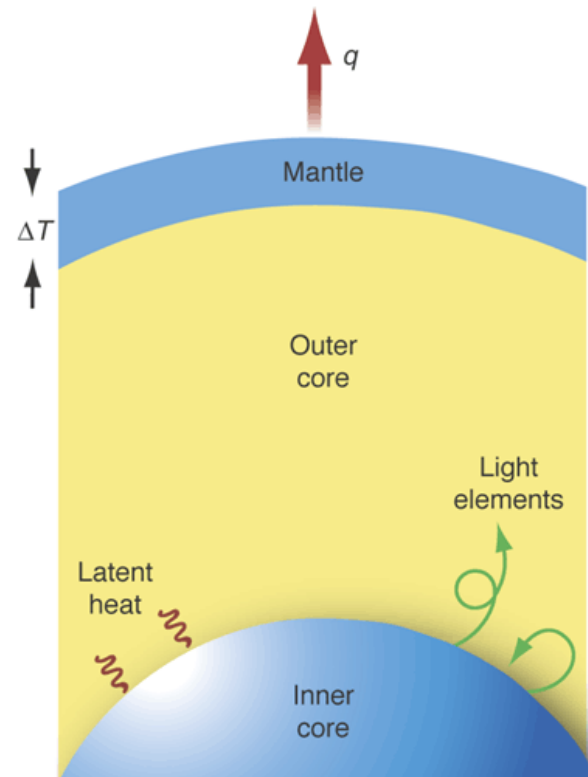
- Magnetic field generation easily overcomes dissipation - **dynamo!**
- **Frozen-flux limit:** On short timescales and large lengthscales diffusion is negligible and the **field** acts as a **tracer**, i.e. ‘frozen’, carried by the flow.

4. Dynamo theory - Necessary ingredients for a dynamo

Dynamo requires Rm larger than a critical value:

- **Electrically-conducting fluid** - small λ .
- Energy source - large U . In planetary cores energy supplied by **thermal** (CMB heat flux) and **compositional** (light element release due to inner core freezing) **convection**.
- Efficient field generation - low critical magnetic Reynolds number Rm_c . **Rotation** organizes flow in favorable morphology for a dynamo.

$$Rm = \frac{UD}{\lambda}$$



4. Dynamo theory - generation mechanisms

Generation of poloidal field from toroidal field and vice-versa via the α -effect (Olson et al., 1999).

Helicity important for dynamo action:

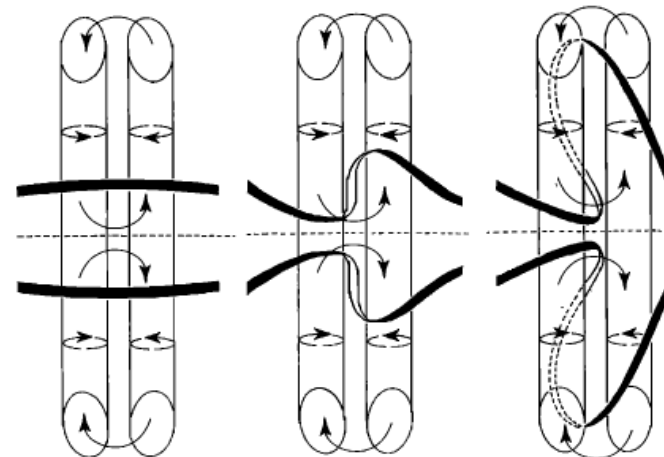
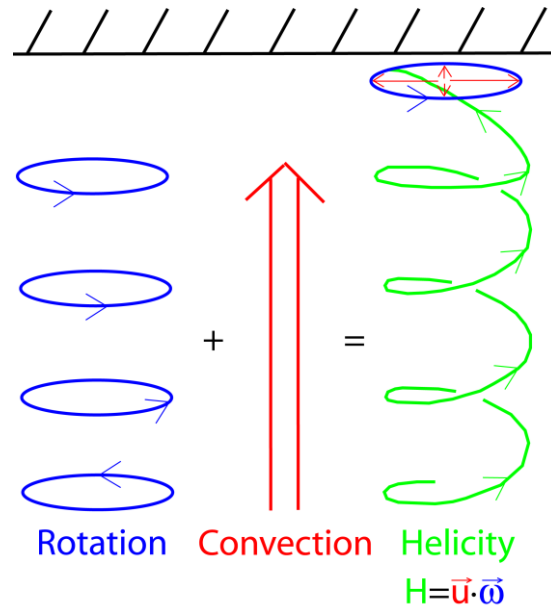


Figure 5a. Schematic illustration of the generation of poloidal field from initial toroidal field by columnar convection. Small arrows indicate the primary (columnar) flow and larger arrows indicate the secondary circulation along the column axes and between columns.

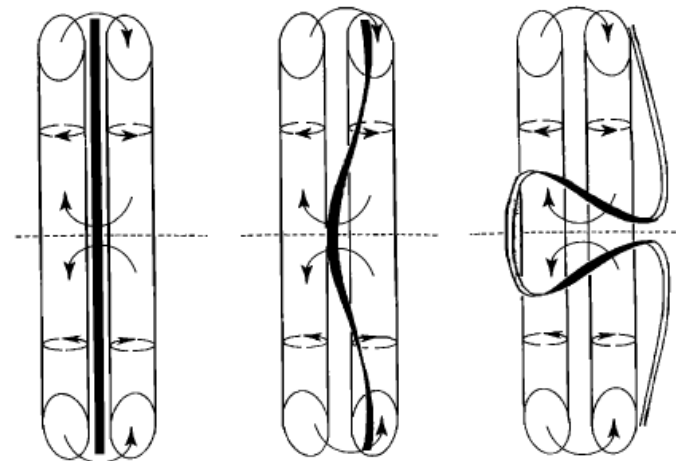
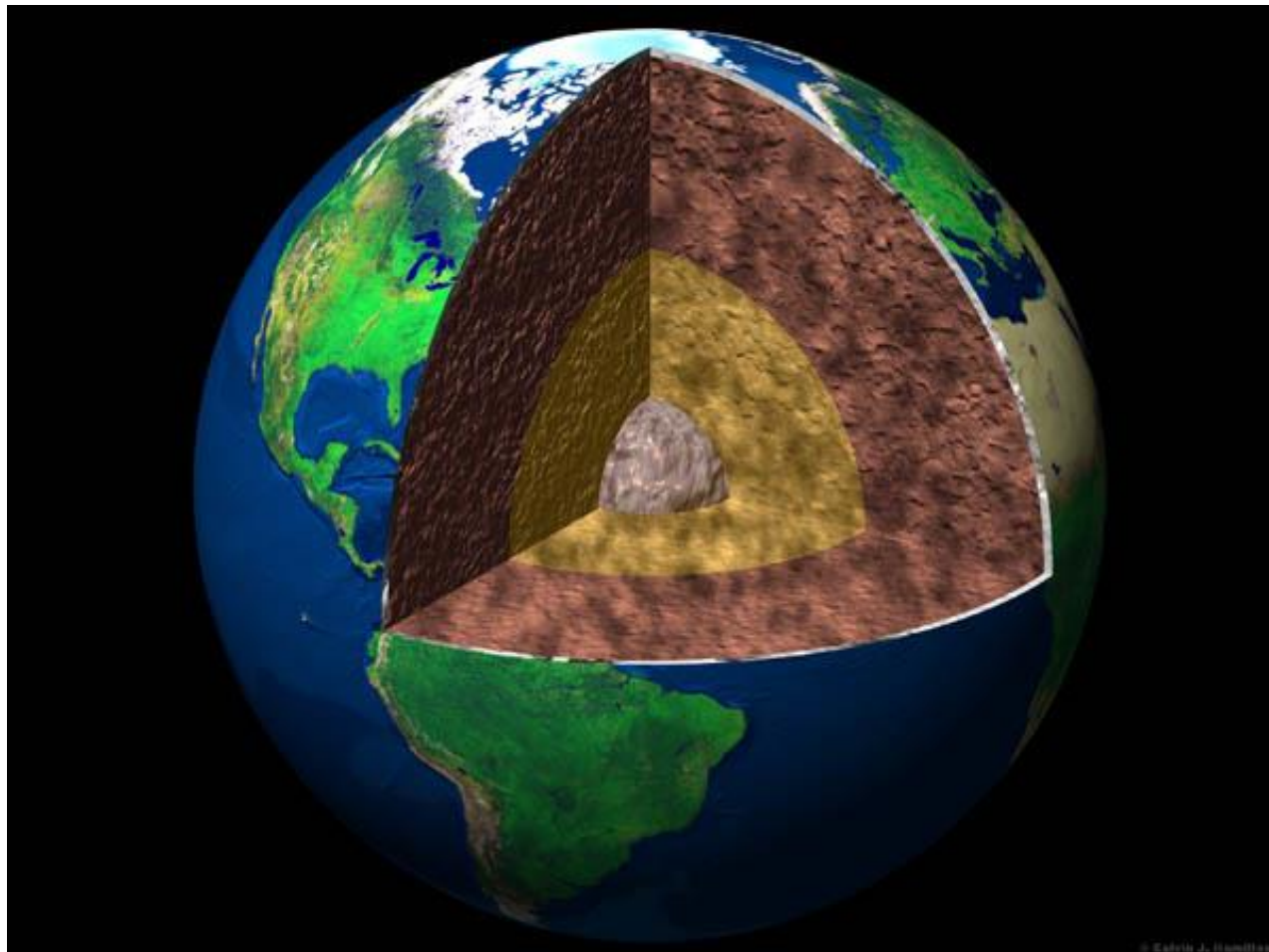


Figure 5b. Schematic illustration of the generation of toroidal field from initial poloidal field by columnar convection.

5. Observations - radial seismic profile

From seismology:

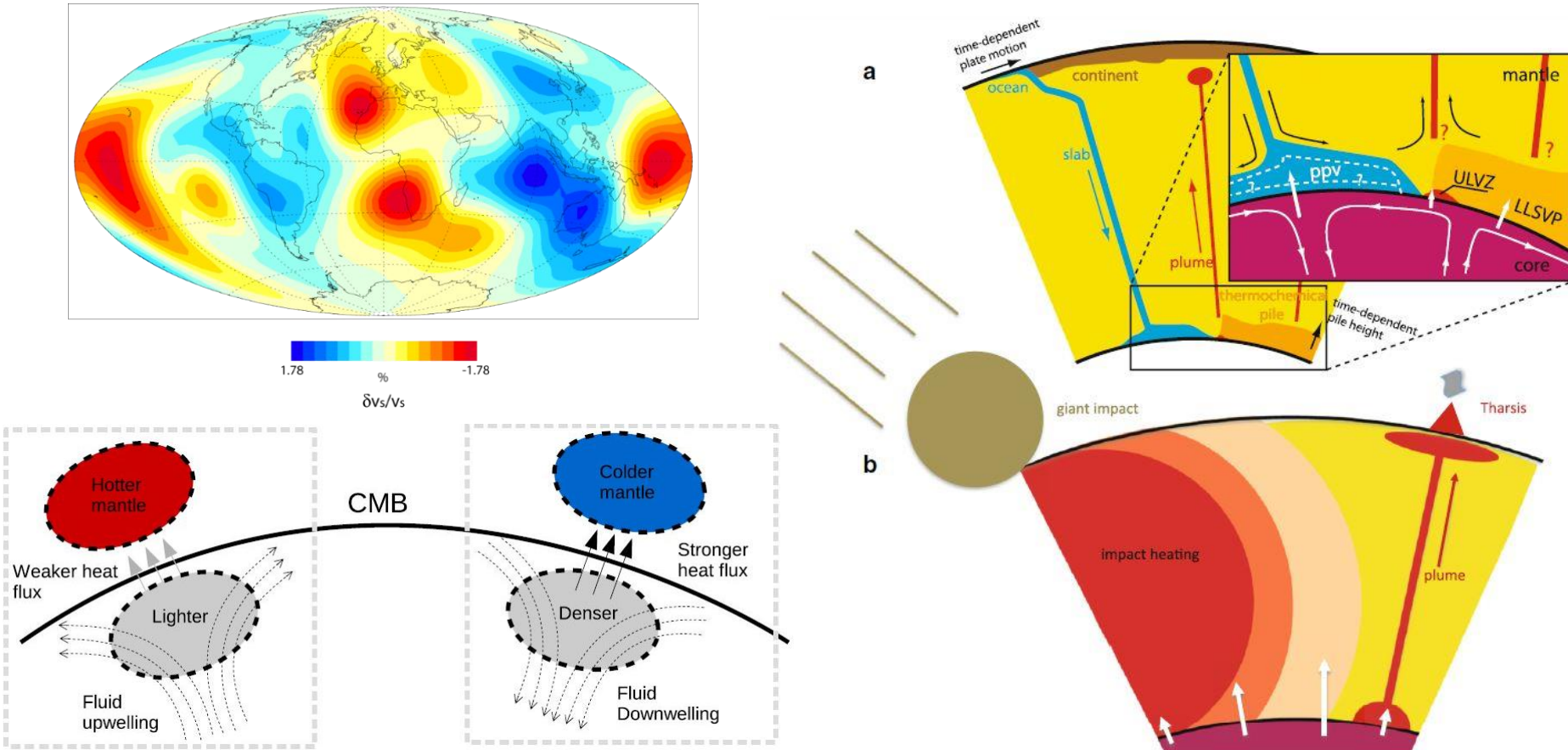
- Solid, insulating mantle.
- Liquid, electrically-conductive outer core - dynamo region.
- Solid, electrically-conductive inner core - freezing an energy source for the dynamo.



5. Observations - lateral seismic anomalies above CMB

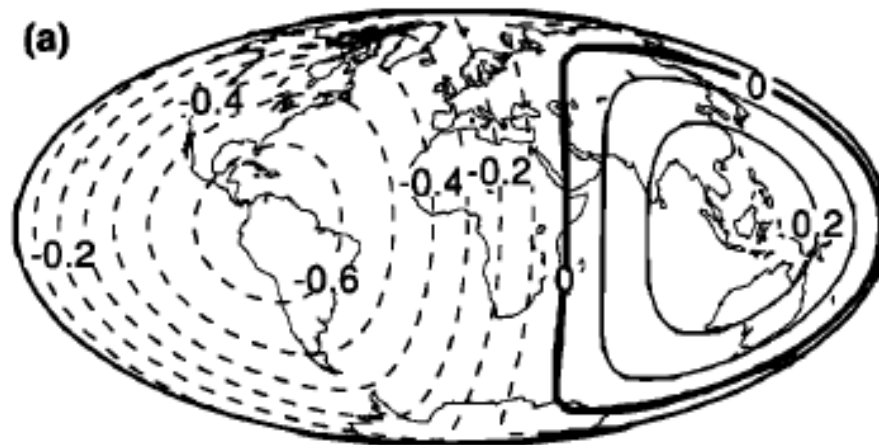
The lowermost mantle is the most laterally heterogeneous part of Earth. D'' seismic anomalies (Masters et al., 2000) have been used to assess CMB heat flux pattern (e.g. Amit et al., 2015).

Cold mantle → large CMB heat flux → cold core → core downwelling below the CMB → intense magnetic flux patch on the CMB (e.g. Terra-Nova et al., 2019).



5. Observations - lateral seismic anomalies below ICB

- Seismic waves from pole to pole ~3% faster than waves along equatorial paths.
- East-west hemispheric dichotomy in ICB seismic properties (Tanaka and Hamaguchi, 1997) have been used either as a constraint on output of numerical dynamos (Aubert et al., 2008) or as an input bottom boundary condition for numerical dynamos (Aubert et al., 2013).
- Possible inner core super-rotation.

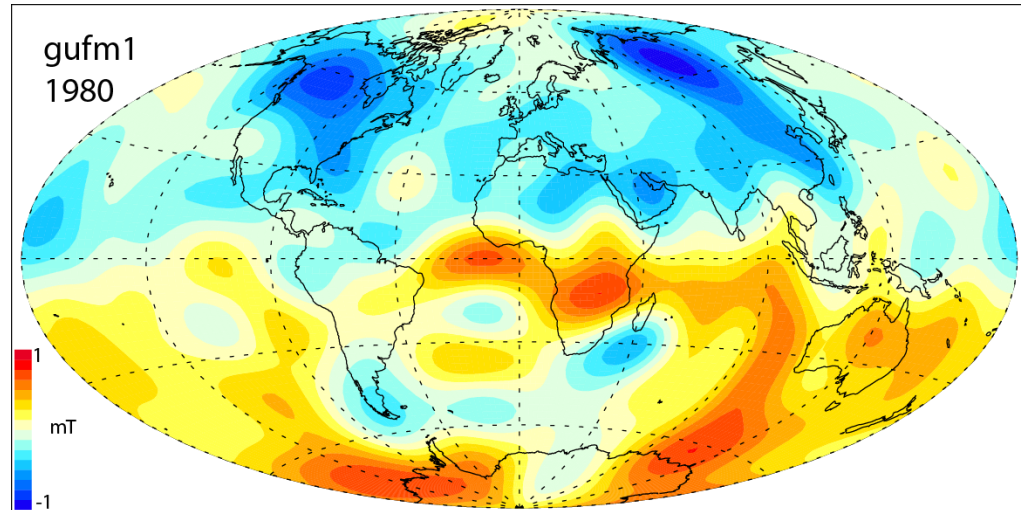
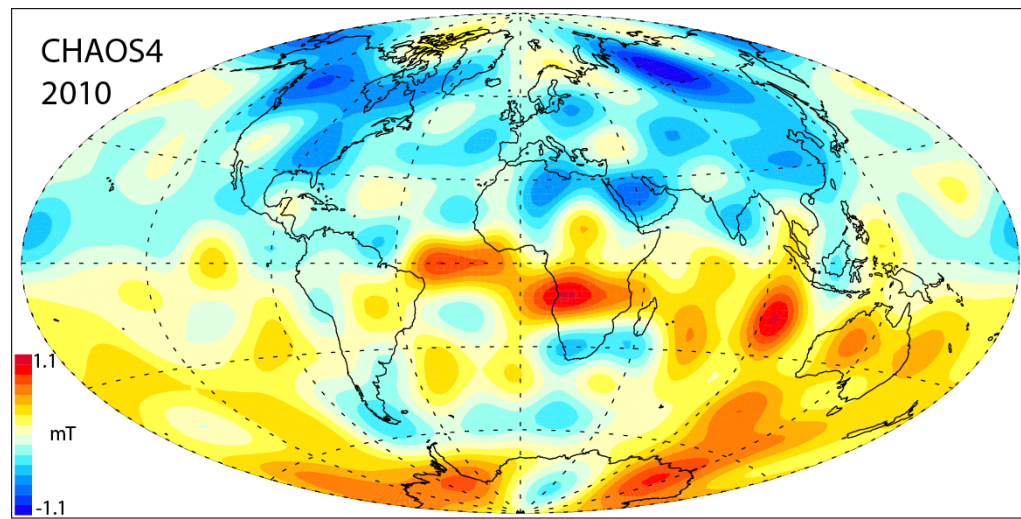


5. Observations - geomagnetic field over various periods

Modern field (1980-present): Direct measurements from satellites and stationary surface observatories (e.g. Olsen et al., 2014). Satellites give full coverage.

Historical field (1590-1990): Direct measurements from stationary surface observatories and ship logs (e.g. Jackson et al., 2000). Prior to 1840 (Gauss) no intensity.

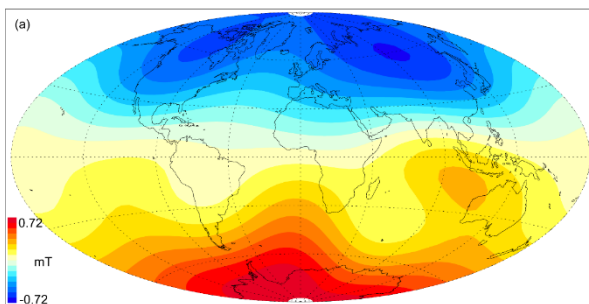
Field and SV features: Axial dipole dominance, high-latitude intense flux patches (2 at each hemisphere), emerging reversed flux patches (mostly below South Atlantic), low- and mid-latitudes westward drift.



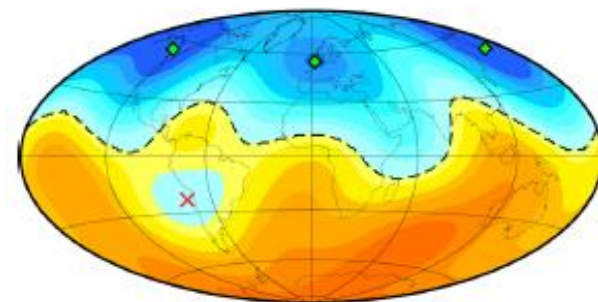
5. Observations - geomagnetic field over various periods

Archeomagnetic field (past millennia): Indirect measurements from archeological material (e.g. Korte and Constable, 2011; Licht et al., 2013; Hellio and Gillet, 2018). Similar features as in recent field (e.g. Terra-Nova et al., 2016) though much lower spatio-temporal resolution due to much lower data quantity and reliability.

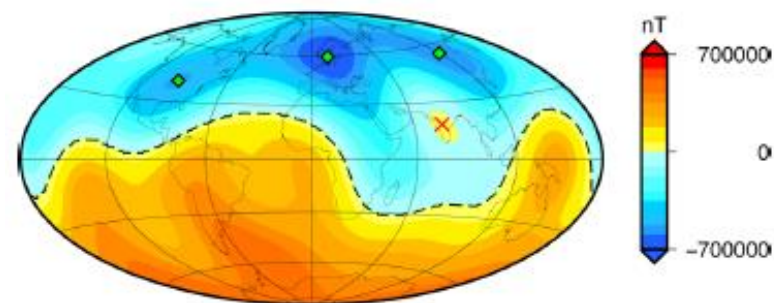
Paleomagnetic field (time-average past 5 Myrs): Debatable whether **non-zonal** features are robust. If yes (Kelly and Gubbins, 1997), evidence for boundary control.



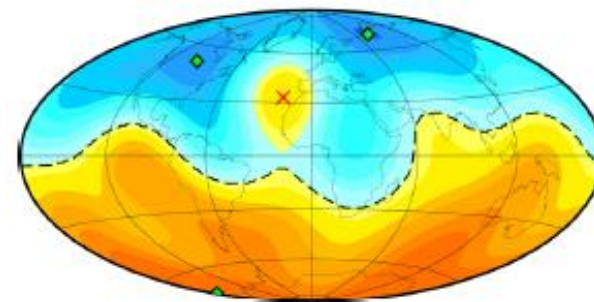
(a) A_FM-M 0160BC



(b) A_FM-M 0920AD

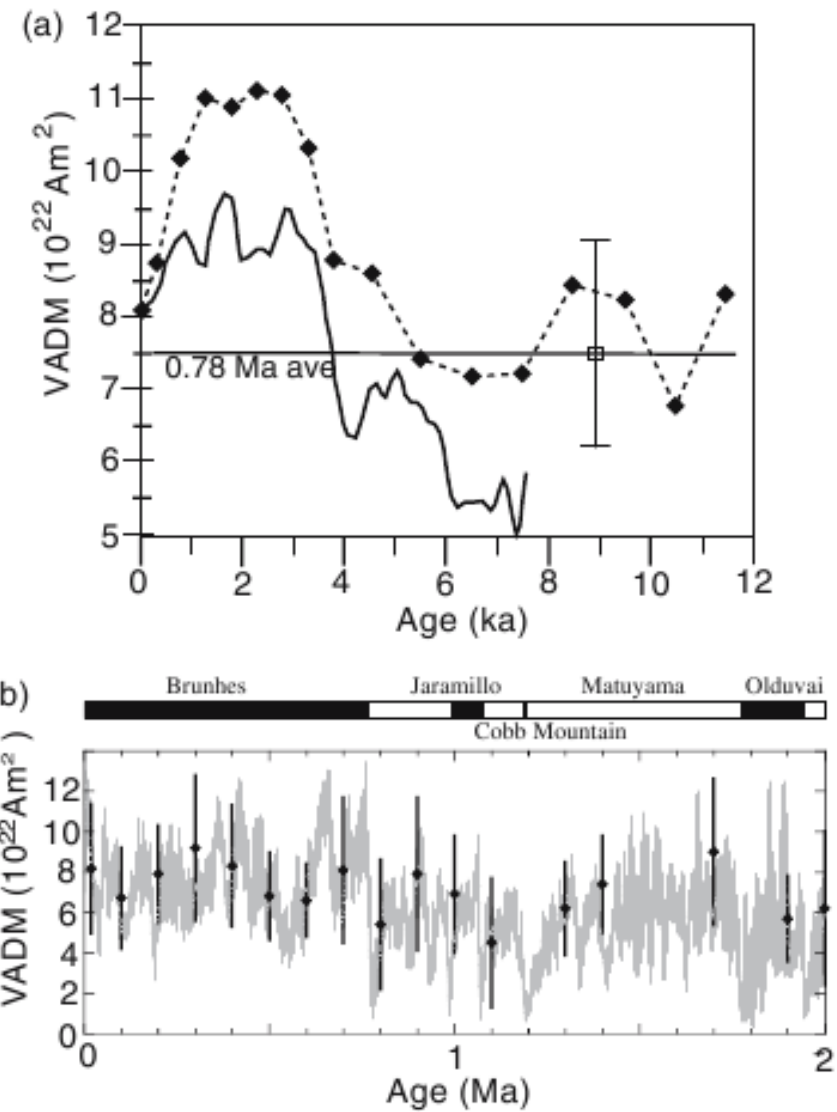
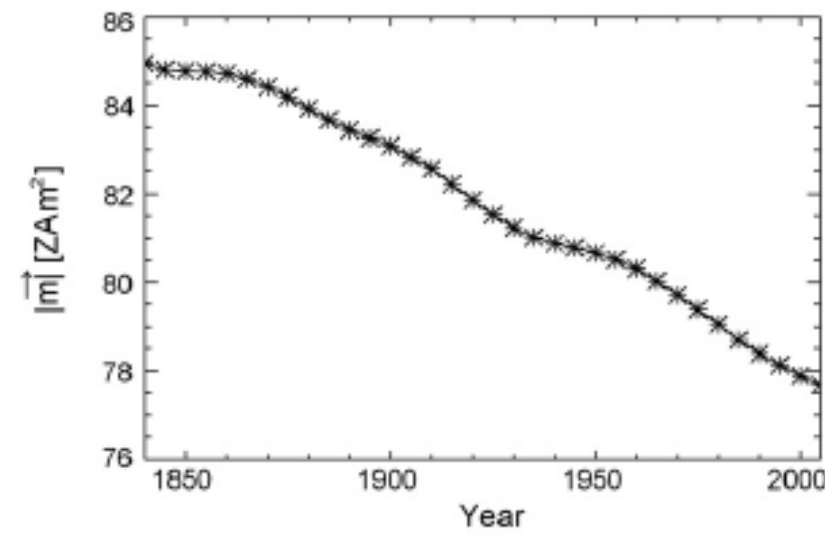


(c) A_FM-M 1520AD



5. Observations - geomagnetic intensity

Rapid decrease in dipole moment strength since 1840 - a beginning of a reversal? Present dipole intensity larger than long-term time-average, and many events of rapid decrease that did not end in a reversal have occurred in Earth's history (Olson and Amit, 2006; Brown et al., 2018).



5. Observations - downward projection

Need to project measurements from the surface (or from space) **to the CMB**.

Above the CMB potential field: $\vec{J} = 0 \Rightarrow \nabla \times \vec{B} = 0 \Rightarrow \vec{B} = -\nabla V$

Everywhere: $\nabla \cdot \vec{B} = 0$

Laplace's equation for the magnetic potential: $\nabla^2 V = 0$

Analytical solution in spherical coordinates (separation of variables):

$$V = a \sum_{n=1}^m \sum_{m=0}^n \left(\frac{a}{r} \right)^{n+1} p_n^m(\cos \theta) (g_n^m \cos(m\phi) + h_n^m \sin(m\phi))$$

$$B_\phi = -\frac{1}{r \sin \theta} \frac{\partial V}{\partial \phi}$$

$$B_\theta = -\frac{1}{r} \frac{\partial V}{\partial \theta}$$

$$B_r = -\frac{\partial V}{\partial r}$$

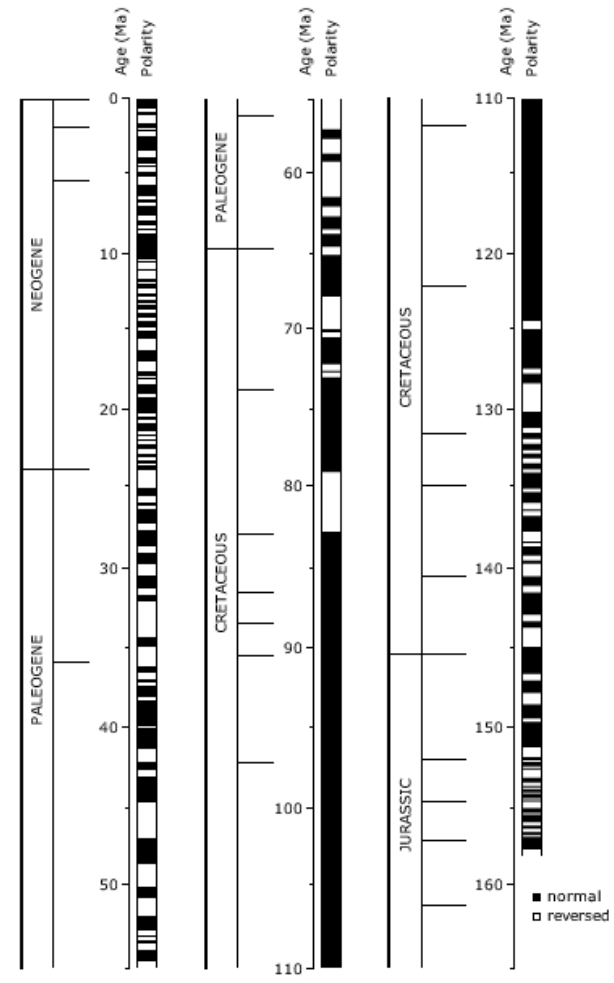
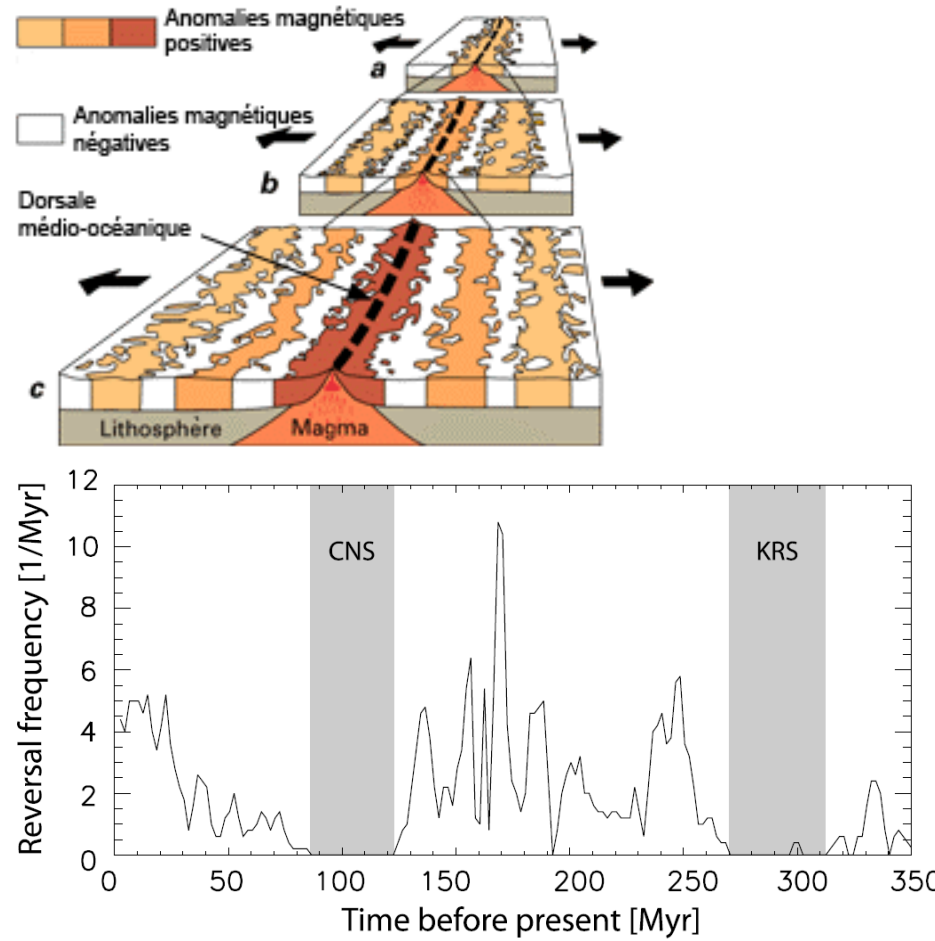
Spherical harmonics:

- $n=1$ dipole, $n>1$ non-dipole.
- $m=0$ axial (zonal), $m>0$ non-zonal (longitude dependent).
- $n+m$ even/odd equatorially symmetric/antisymmetric.

Measurements include core + crustal fields. Truncate at $n \sim 14$ to remove crustal field.

5. Observations - reversals

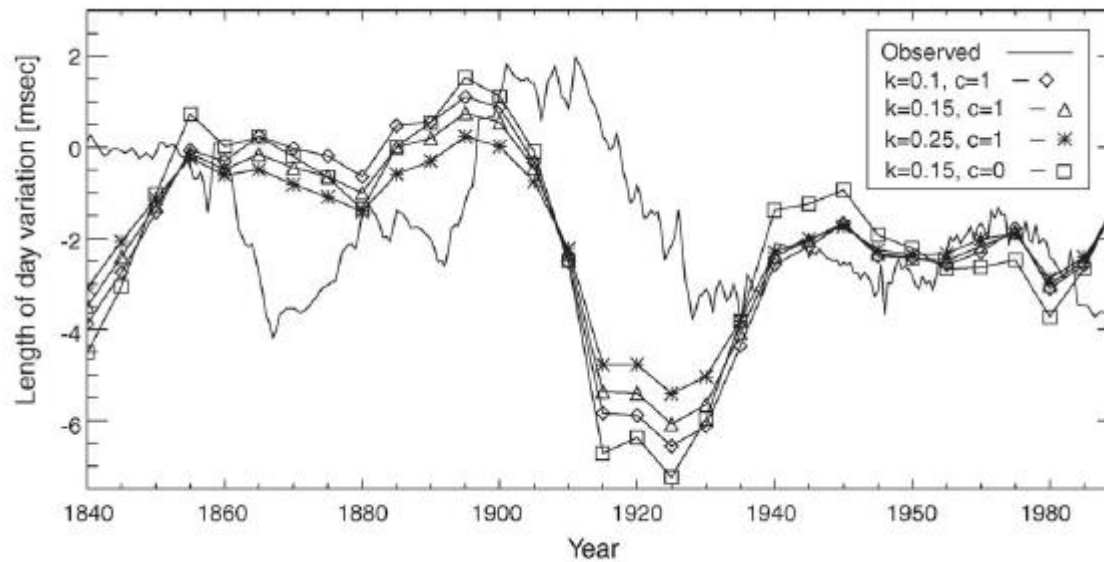
- Mid ocean ridges show symmetric polarity pattern corresponding to reversal history of over the past 180 Myrs (Gradstein et al., 2012).
- Average chron ~250 kyr, average reversal ~10 kyr, **very rapid events!**
- **Very irregular** frequency, including **superchrons** (CNS=40 Myrs) and **hyper-reversing** (~40 kyr) - chaotic core dynamics or changes in mantle convection?



5. Observations - length of day

Less than a year - atmosphere and oceans. Geological timescales - changes in moment of inertia of the mantle. **Decadal-centennial length of day variations correspond to changes in mantle rotation rate.**

Conservation of angular momentum in core-mantle system constrains time-dependence of **core flow** (e.g. Amit and Olson, 2006).



5. Observations - planetary magnetic fields

- Mars had a dynamo but not anymore (crustal field model from Langlais et al., 2004). Why did the **Martian dynamo die?**
- Venus possibly never had a dynamo - why?
- Mercury has a very weak field, strongly axisymmetric, strongly hemispheric** (Thébault et al., 2018).

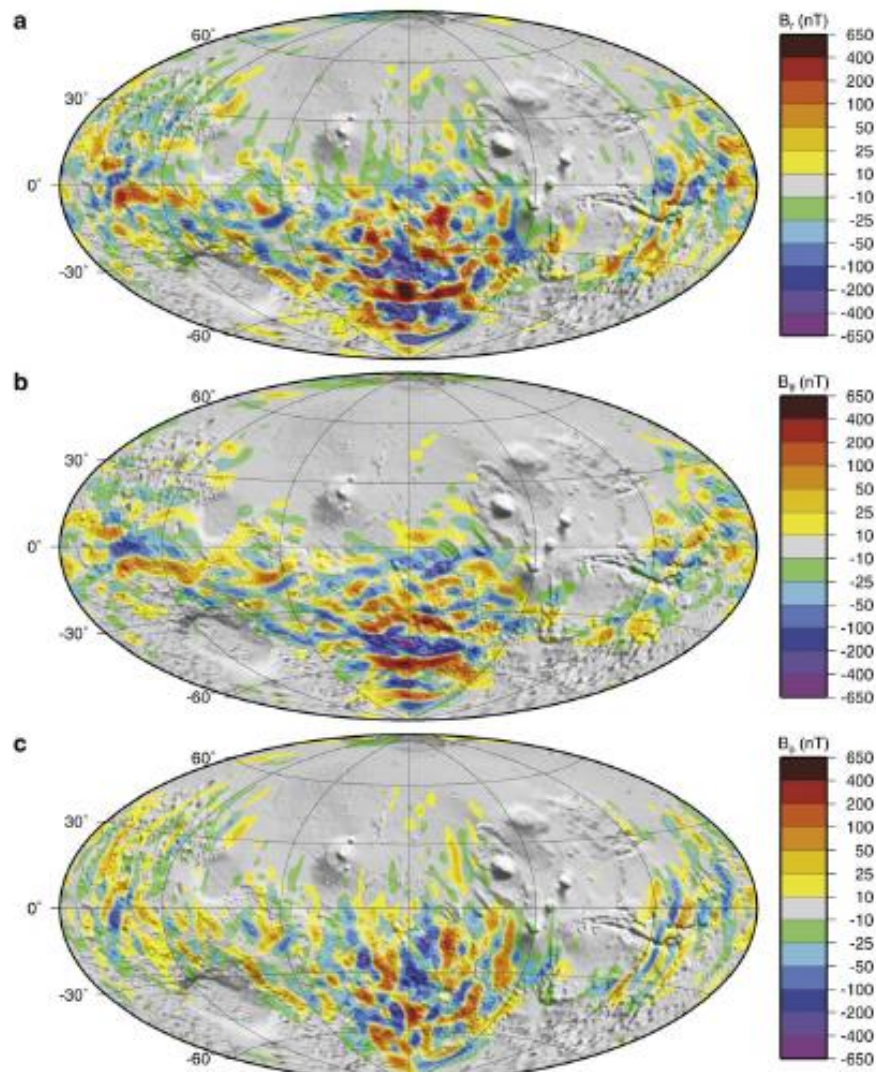
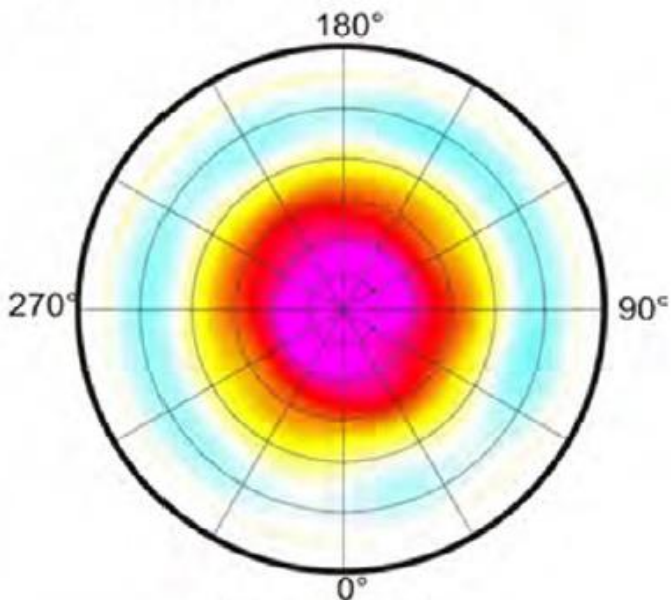
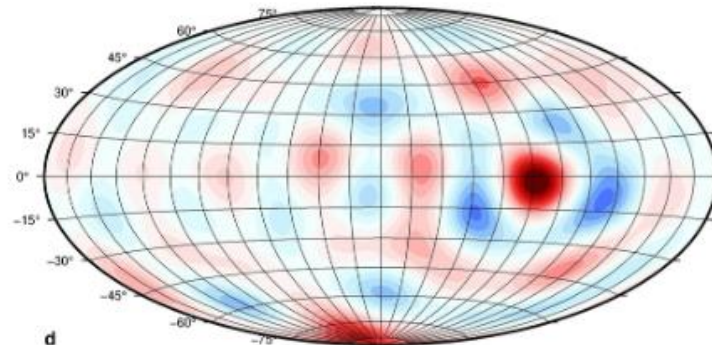
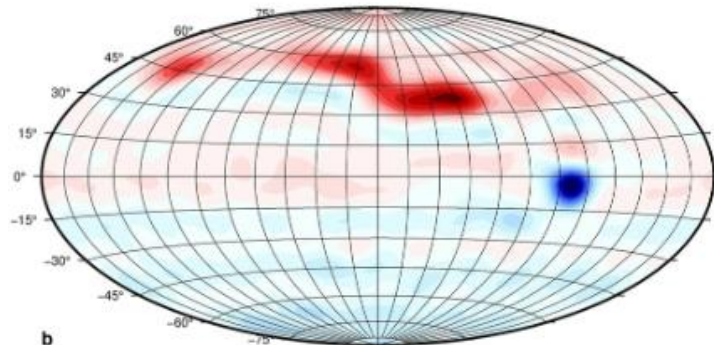


Figure 4. Predicted magnetic field at 200-km altitude, from M23/-20/14.

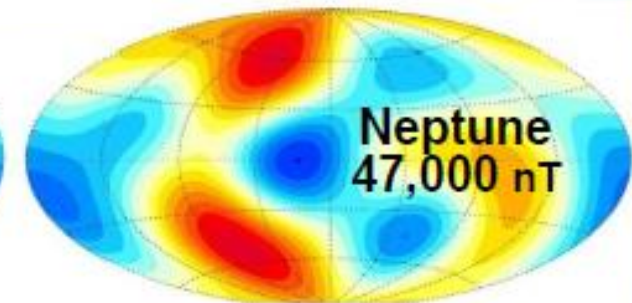
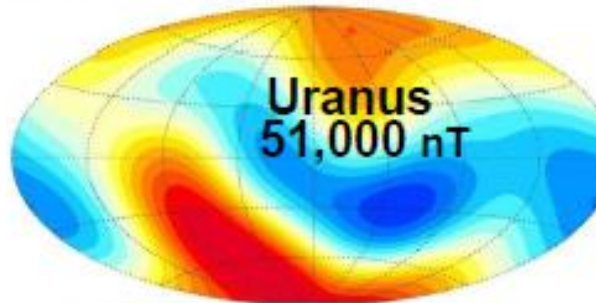
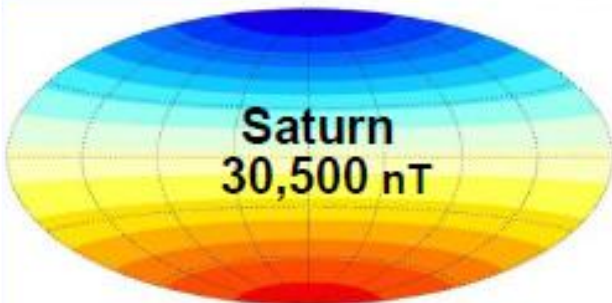
5. Observations - planetary magnetic fields

- Earth and Jupiter fields are dipole-dominated with similar tilts, but Jupiter's field is hemispherical.



Radial field (left) and SV (right) at the top of Jupiter's dynamo region (Sharan et al., 2022).

- Saturn field perfectly axisymmetric, contradicts Cowling's theorem.
- Uranus and Neptune fields are non-dipolar, non-axial (Holme and Bloxham, 1996).



6. Core flow inversions - theory

Of the seven dynamo parameters (field vector, flow vector, co-density) in 3D **only** the radial field on the CMB is observed - need more!

$$\frac{\partial \vec{B}}{\partial t} = \nabla \times (\vec{u} \times \vec{B}) + \lambda \nabla^2 \vec{B}$$

Assume frozen-flux:

$$\frac{\partial \vec{B}}{\partial t} = \nabla \times (\vec{u} \times \vec{B})$$

Apply no monopoles and continuity:

$$\frac{\partial \vec{B}}{\partial t} - (\vec{B} \cdot \nabla) \vec{u} + (\vec{u} \cdot \nabla) \vec{B} = 0$$

Take radial component (assume no radial flow below the CMB):

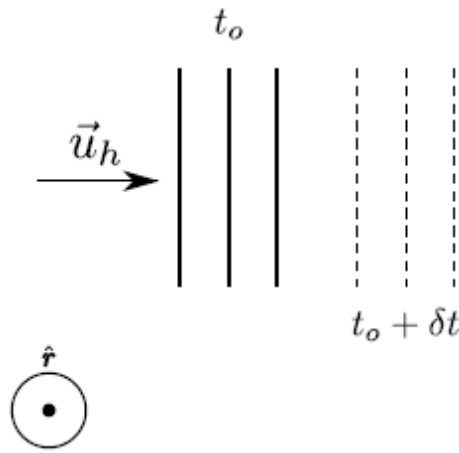
$$\frac{\partial B_r}{\partial t} + \vec{u}_h \cdot \nabla B_r + B_r \nabla_h \cdot \vec{u}_h = 0$$

6. Core flow inversions - theory

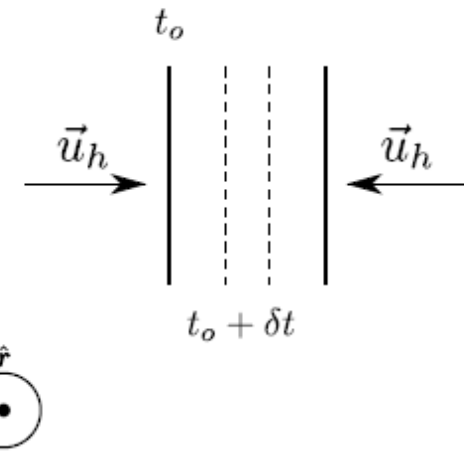
$$\frac{\partial B_r}{\partial t} + \vec{u}_h \cdot \nabla B_r + B_r \nabla_h \cdot \vec{u}_h = 0$$

advection stretching

a) Ad_h



b) St_h



Frozen-flux SV is due to **advection** of radial field by the tangential flow (analogous e.g. to heat advection) and **stretching** of radial field by the poloidal flow (illustration from Peña et al., 2018).

6. Core flow inversions - theory

$$\frac{\partial B_r}{\partial t} + \vec{u}_h \cdot \nabla B_r + B_r \nabla_h \cdot \vec{u}_h = 0$$

advection stretching

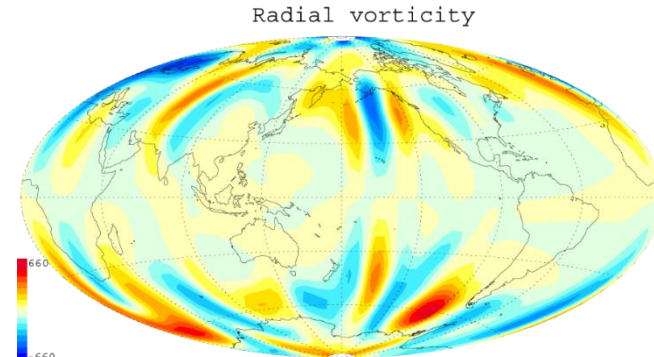
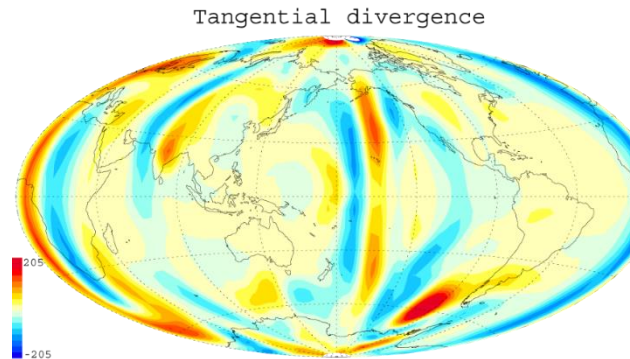
Forward problem: Given \vec{u}_h and B_r find $\partial B_r / \partial t$ - always possible to reach a **unique** solution.

Inverse problem: Given B_r and $\partial B_r / \partial t$ find \vec{u}_h - one equation (radial induction) with two variables (two tangential flow components or potentials), inherent **non-uniqueness!**

6. Core flow inversions - physical assumptions

Removing (or reducing) non-uniqueness needs an additional **physical assumption**:

- Pure toroidal flow (Whaler, 1980): Assume $\nabla_h \cdot \vec{u}_h = 0$ i.e. no upwelling, no stretching SV. May correspond to stratified top of the core. Pros: Economical, toroidal flow dominant in most core flow models. Cons: Difficult to explain intense flux concentration, emergence of reversed flux, dipole decrease...
- Tangential geostrophy (LeMouël, 1984): From the radial component of Taylor-Proudman assume $\nabla_h \cdot (\vec{u}_h \cos \theta) = 0$ i.e. should correspond to rapid rotation conditions. Pros: Based on a reasonable approximated force balance. Cons: Equatorial singularity of upwelling.
- Helical flow (Amit and Olson, 2004): Assume $\nabla_h \cdot \vec{u}_h = \mp k\omega_r$ from **numerical dynamos**. Pros: Typical to rotating-convecting systems, helicity essential for dynamos. Cons: Discontinuous at equator.



6. Core flow inversions - physical assumptions

- Columnar flow (Amit and Olson, 2004): Combine Taylor-Proudman and non-parallel boundaries of spherical shell for a column parallel to the rotation axis gives $\nabla_h \cdot (\vec{u}_h \cos^2 \theta) = 0$. Similar but not identical to tangential geostrophy (Amit and Pais, 2013).
- Quasi-geostrophy (QG; Pais and Jault, 2008): Assume equatorial symmetry, no flow across tangent cylinder, columnar flow. Pros: Consistent treatment of rapid rotation. Cons: Over-determined.
- Data assimilation (Fournier et al., 2011): Apply statistics from a dynamo model to relate flow with observables. Pros: More sophisticated, flexible, can account for various effects (e.g. magnetic diffusion). Pro and con: Relies on validity of dynamo model.

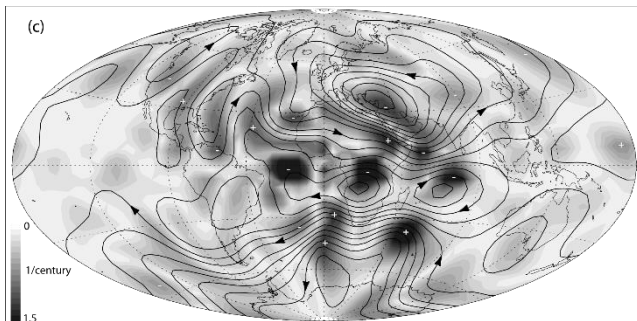
6. Core flow inversions - problems

- Frozen-flux: If diffusion is not fully justified, difficult to incorporate.
- Physical assumption: Which captures best Earth's core?
- Non-uniqueness: Distinctive flows adequately explain observations - **field-aligned flow** produces zero SV.

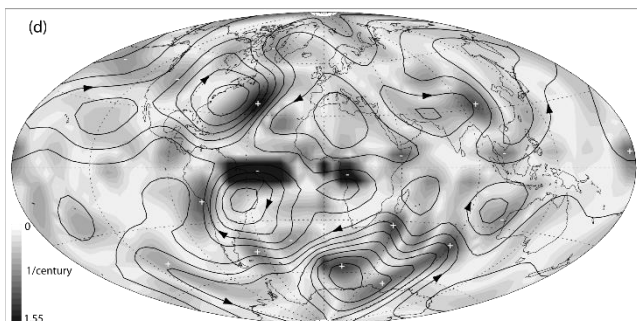
Progress: **Length of day** constrains core flows (Jault et al., 1988). However, this constrains only time-dependent zonal equatorially symmetric flow. **Necessary but not sufficient condition**.

6. Core flow inversions - some (old) solutions

1940



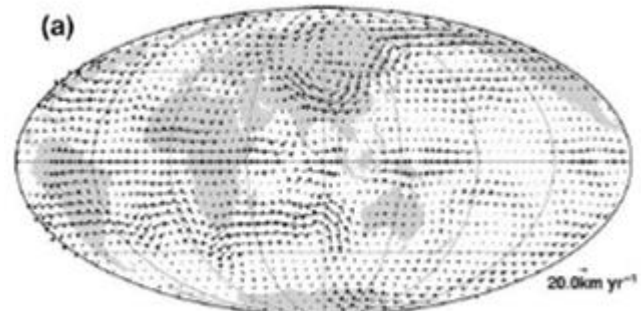
1990



Amit and Olson (2006), helical flow, historical field.

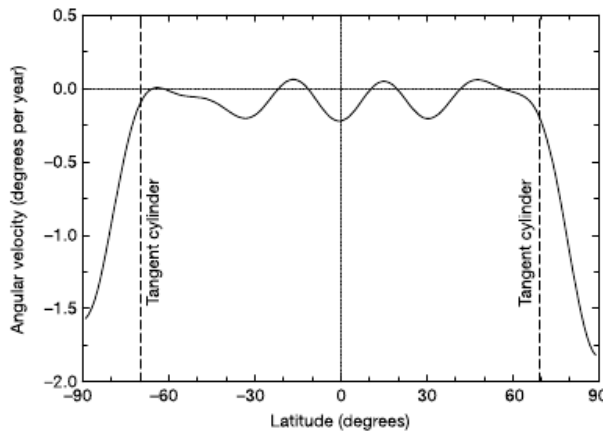
- More intense flow in **Atlantic hemisphere**.
- Large anti-clockwise **gyre** below Atlantic southern hemisphere.
- **Westward drift** at low- and mid- latitudes.

Hulot et al. (2002), tangential geostrophy, satellite field for 1990.

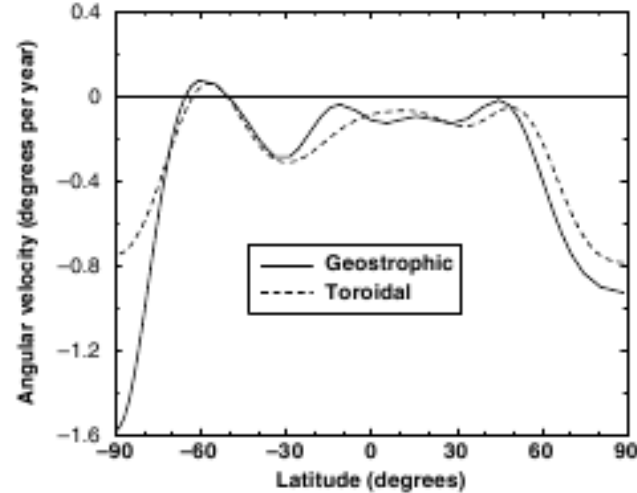


Holme and Olsen (2006), tangential geostrophy (a) and toroidal flow (b), satellite field for 2001.

6. Core flow inversions - zonal profiles



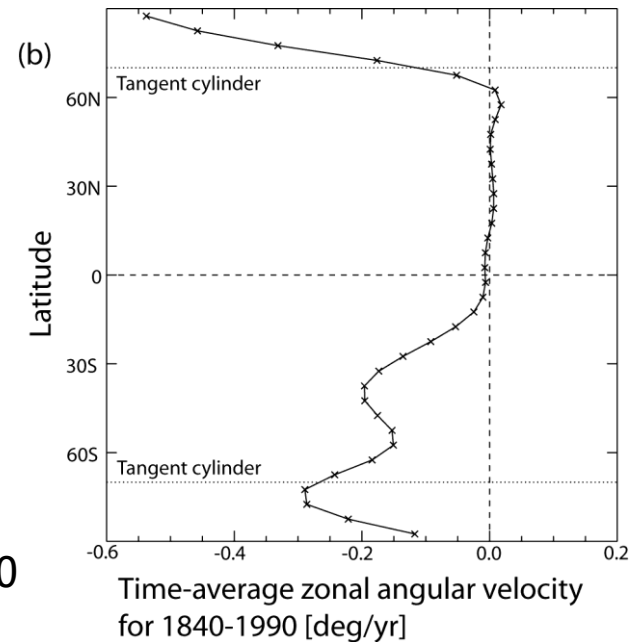
1990 (Hulot et al., 2002).



2001 (Holme and Olsen, 2006).

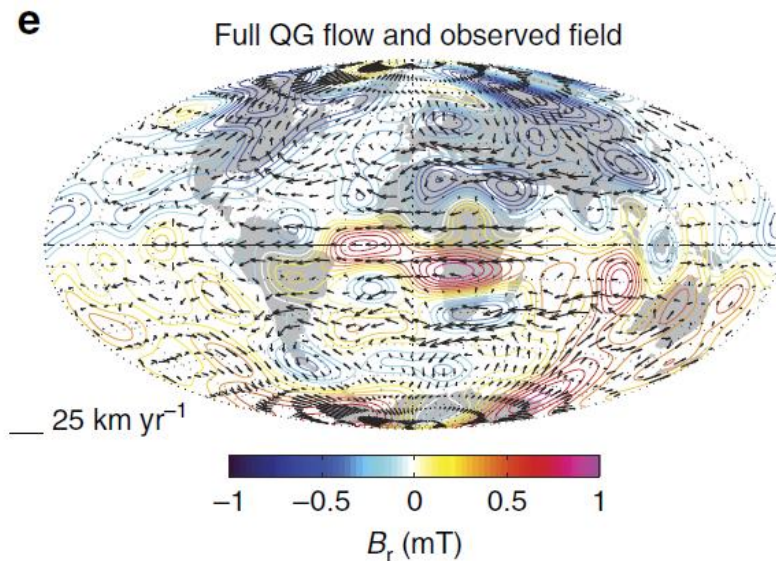
- Westward polar vortices in agreement with thermal wind theory inside tangent cylinder.
- **Stronger westward drift** in southern hemisphere - mantle control?

Time-average 1840-1990
(Amit and Olson, 2006).

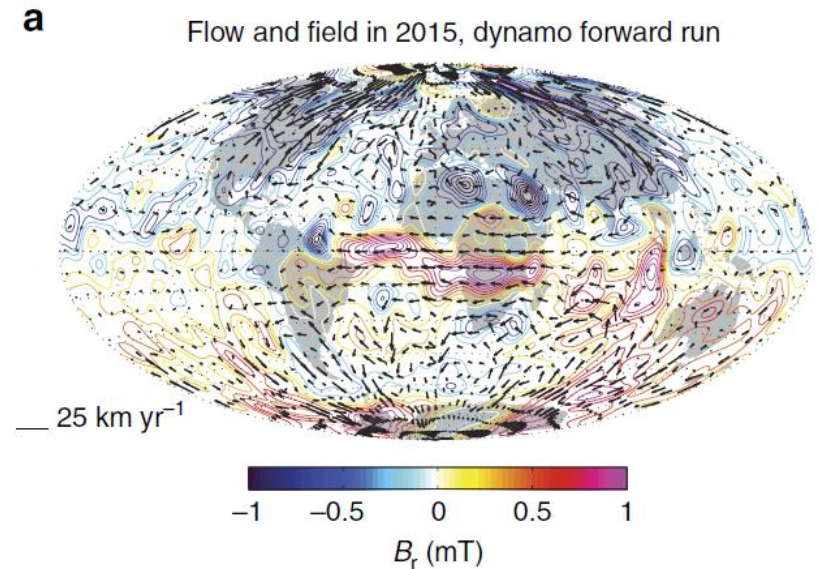


6. Core flow inversions - quasi-geostrophy and data assimilation

Comparison from Finlay et al. (2016):



Quasi-geostrophy time-average 2000-2010 (Gillet et al., 2015).



Data assimilation 2015 (Aubert et al., 2013; Aubert, 2014).

Similarities (e.g. gyre below Atlantic) may indicate validity of underlying assumptions (equatorial symmetry due to dominant rapid rotation effects).

6. Core flow inversions - progress

- **Magnetic diffusion SV larger than expected** from Rm estimates because of the presence of a thin magnetic boundary layer below the CMB (Terra-Nova and Amit, 2020).
- **Subgrid effects** - large-scale SV due to the interactions between small-scale field and large-scale flow and small-scale flow and large-scale field (Pais and Jault, 2008).

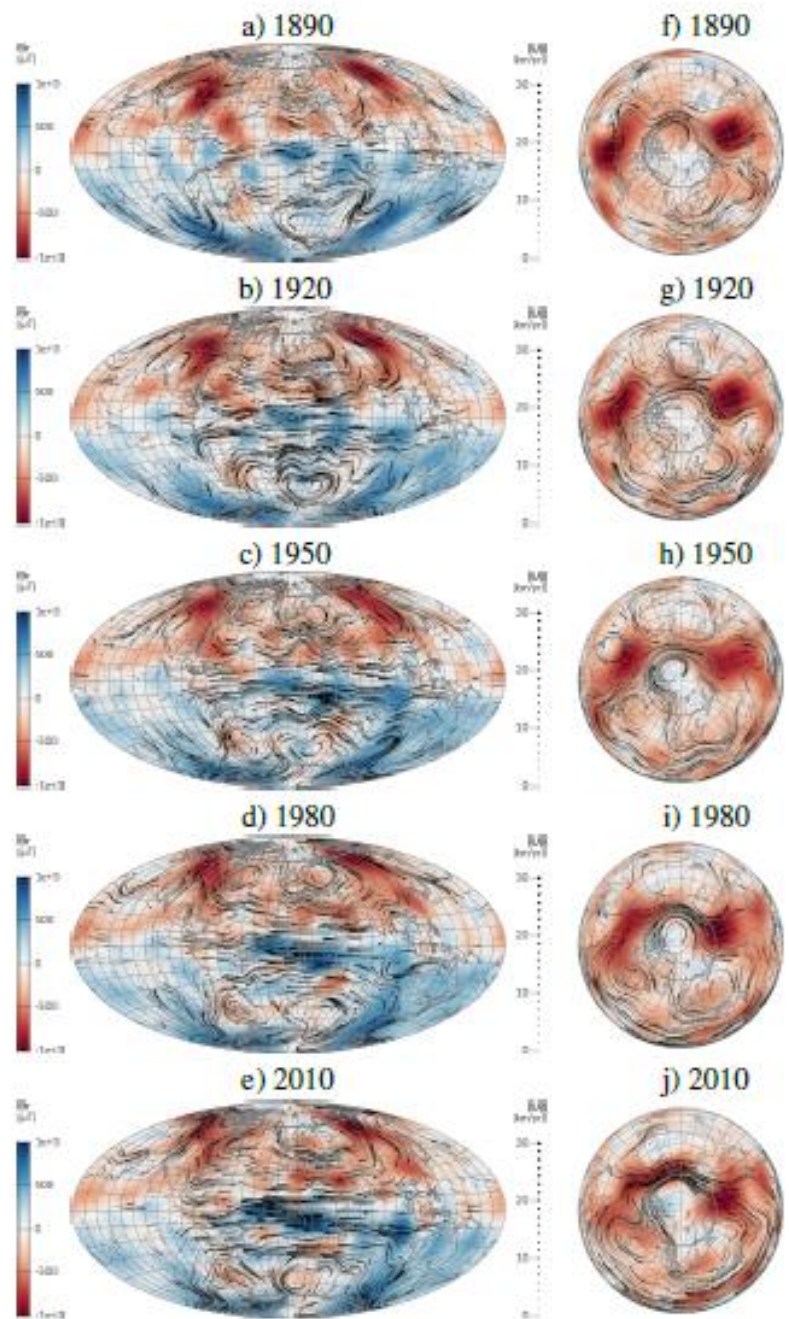
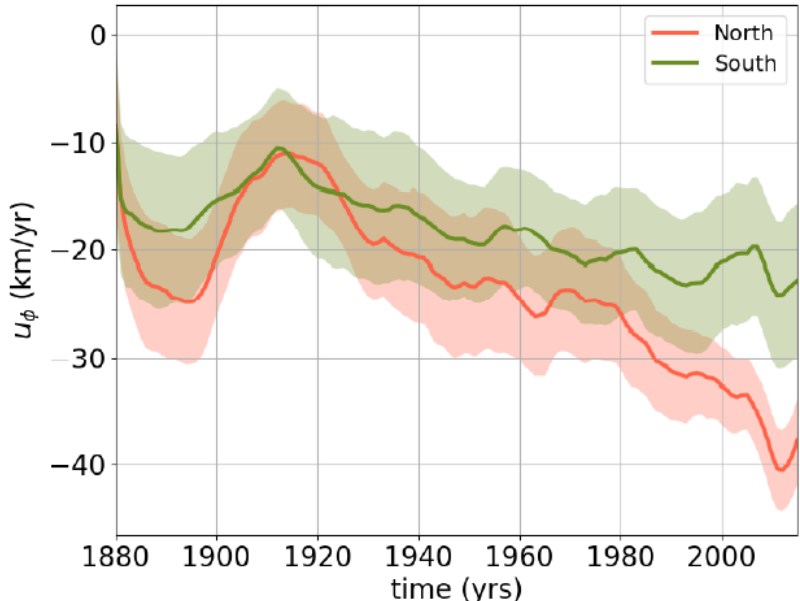
Accounting for magnetic diffusion and sub-grid effects (Gillet et al., 2019):

- **Data assimilation** algorithm derived from a **low E dynamo model** (Aubert et al., 2017).
- Sub-grid effects modelled by an auto-regressive (**stochastic**) process.

6. Core flow inversions - progress

Accounting for magnetic diffusion and sub-grid effects (Gillet et al., 2019):

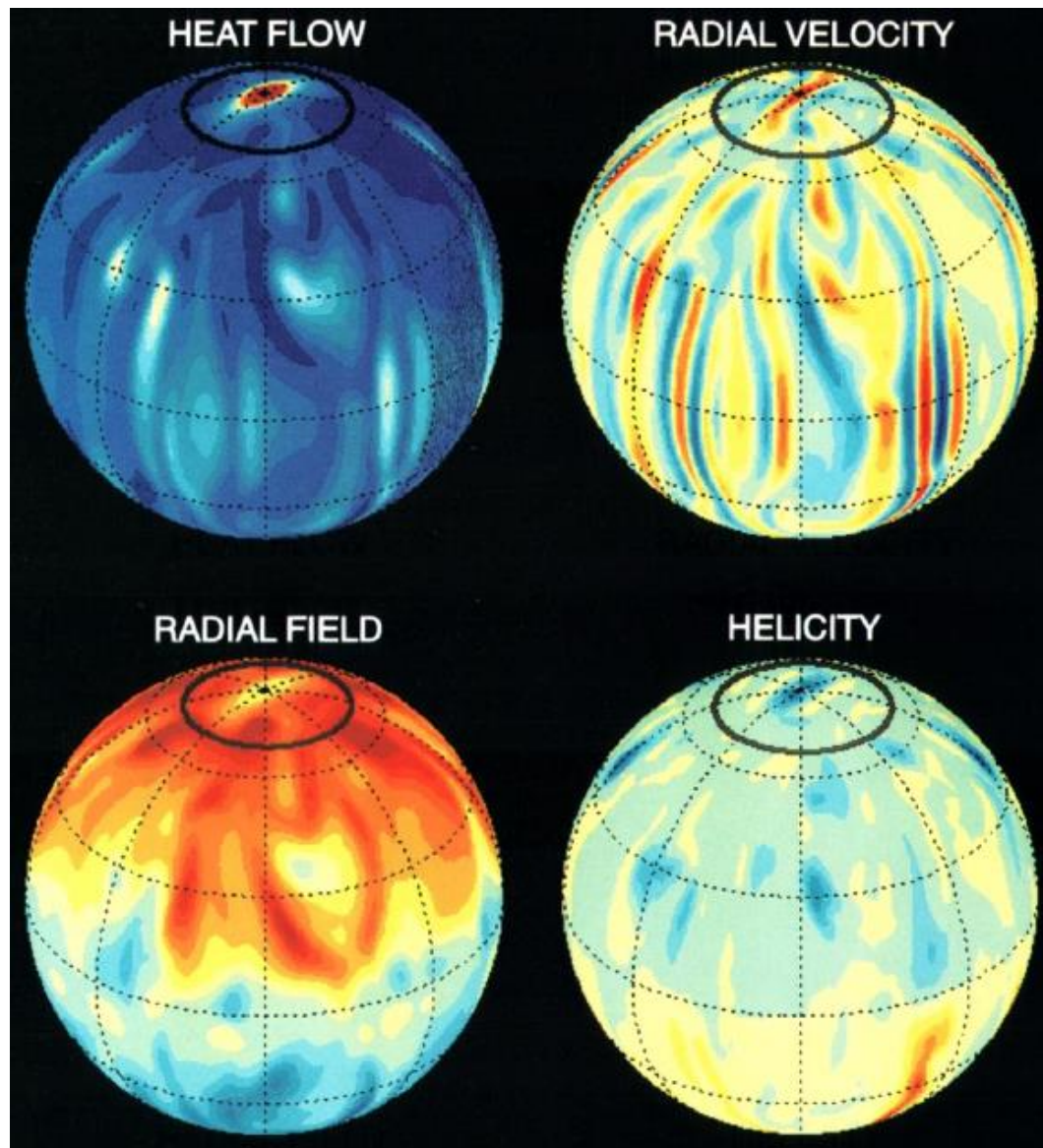
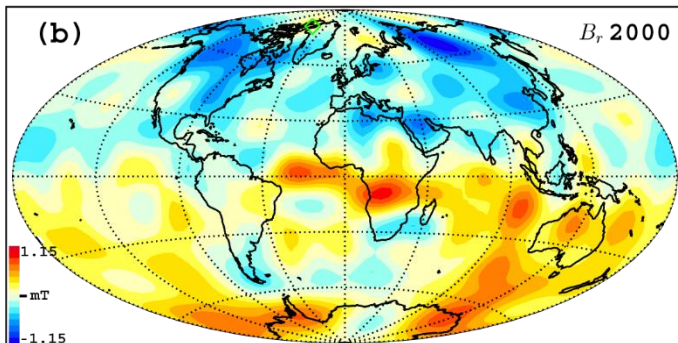
- Eccentric anti-cyclonic gyre (right).
- 90% equatorial symmetry, but high-latitude jet (Livermore et al., 2017) not symmetric (left).
- Large amount of **field-aligned flow** (Finlay and Amit, 2011) - non-uniqueness (problem), but also direct inferences from the field.



7. Numerical dynamos - Earth-like magnetic fields

CMB images from a numerical dynamo model (Olson et al., 1999).

For comparison the geomagnetic field:



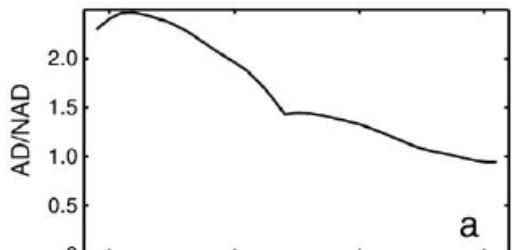
Successes:

- Columnar convection in agreement with QG theory.
- Anti-symmetric helicity efficient in maintaining an alpha-dynamo.
- Axial dipole dominance.
- Intense high-latitude flux patches near tangent cylinder.
- Reversed flux patches at mid-latitudes and at polar regions.

7. Numerical dynamos - Earth-like magnetic fields

Quantitative morphological criteria
from geomagnetic field models
(Christensen et al., 2010):

Dipolarity



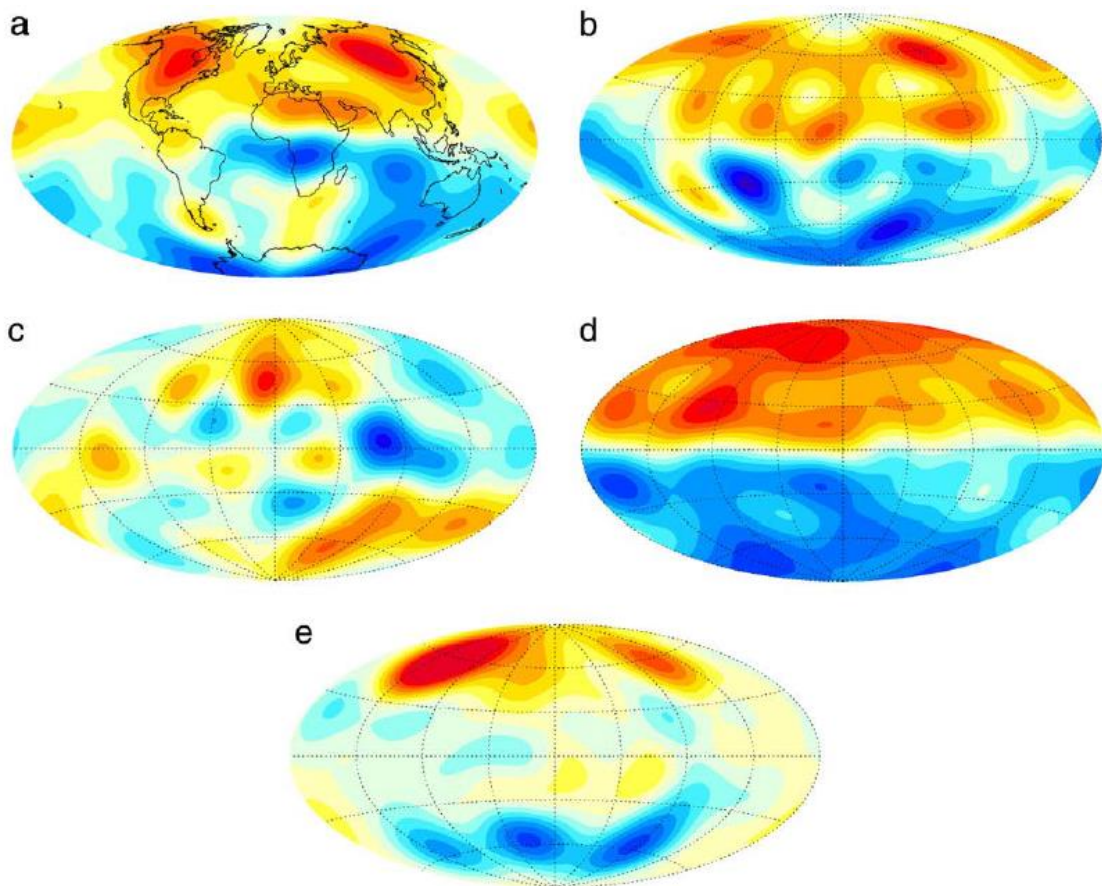
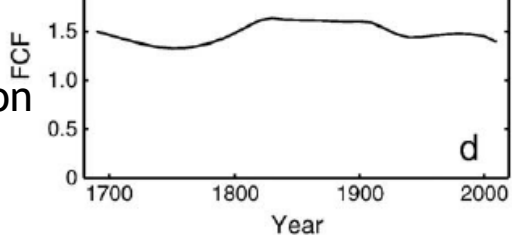
Equatorial Symmetry
(non-dipole)



Zonality
(non-dipole)



Flux concentration^{FCF}

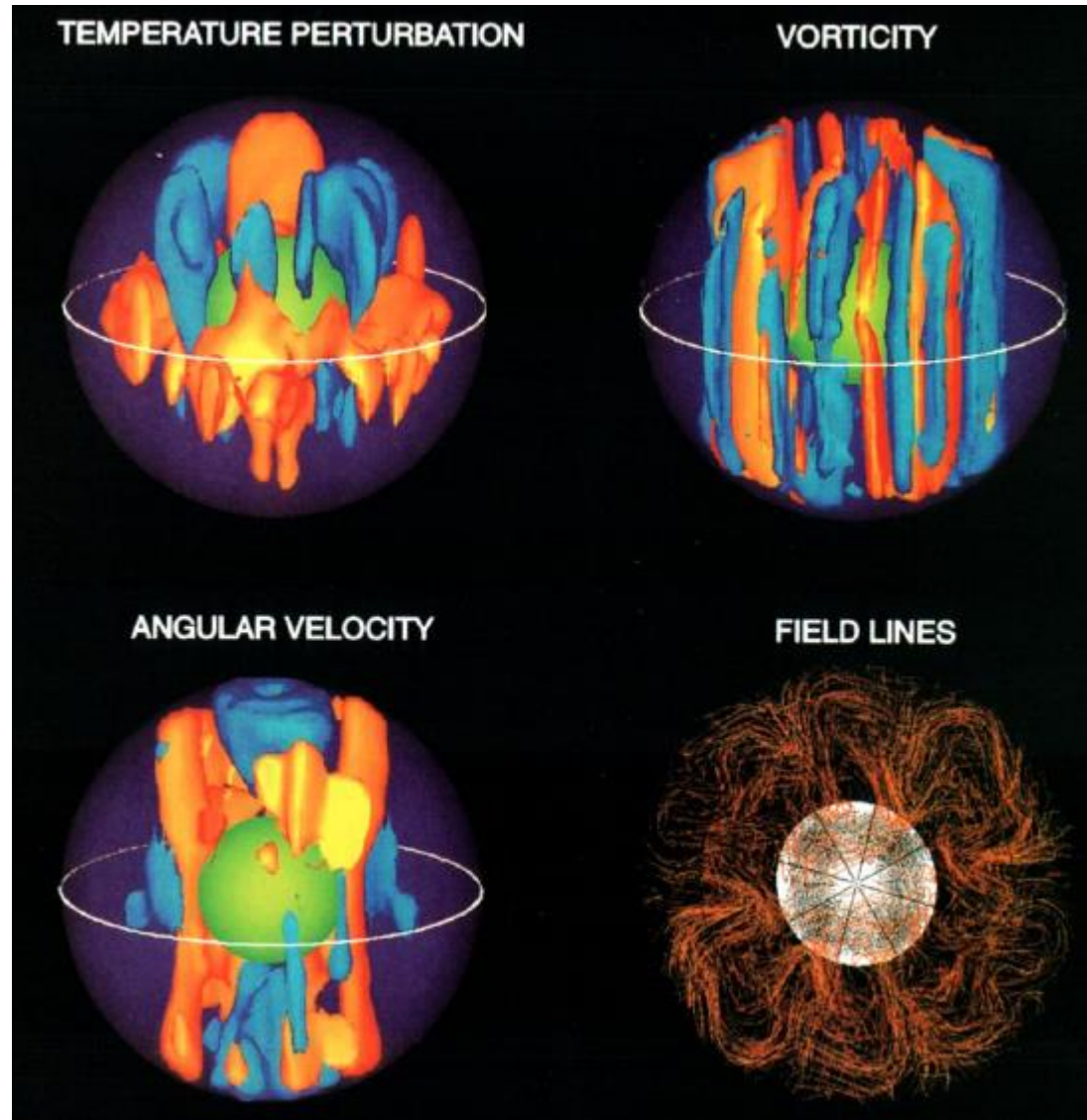


Examples of radial magnetic fields on the outer boundary of four numerical dynamo models (b-e). For comparison Earth's field (a). Case c is non-dipolar. Case d is too dipolar, too equatorially antisymmetric, too zonal and the flux is not concentrated enough. In case e the flux is too concentrated.

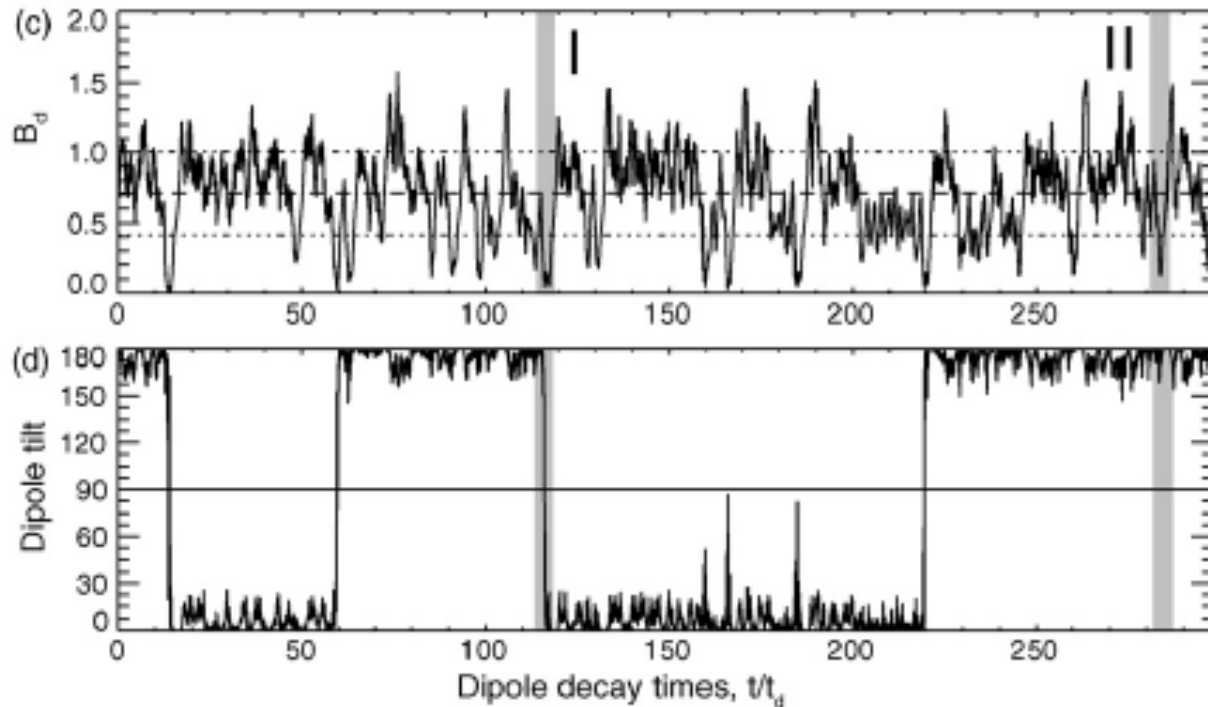
7. Numerical dynamos - a look into the inside

Volume images
demonstrating z-invariance
(Olson et al., 1999).

Problem: No reversals...



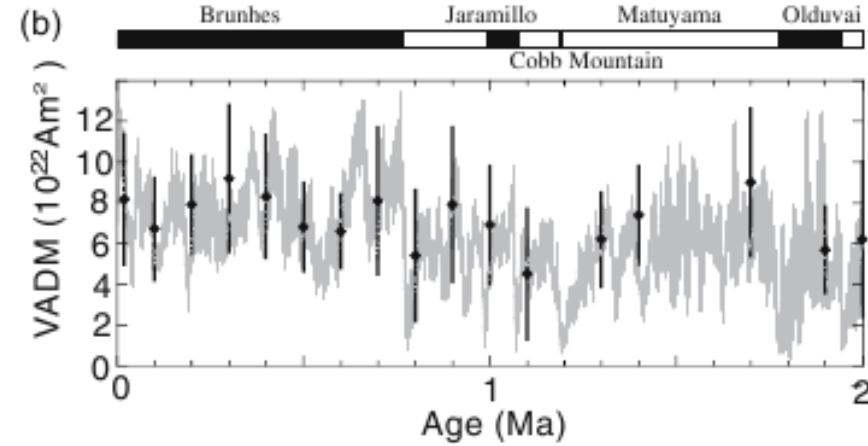
7. Numerical dynamos - reversals



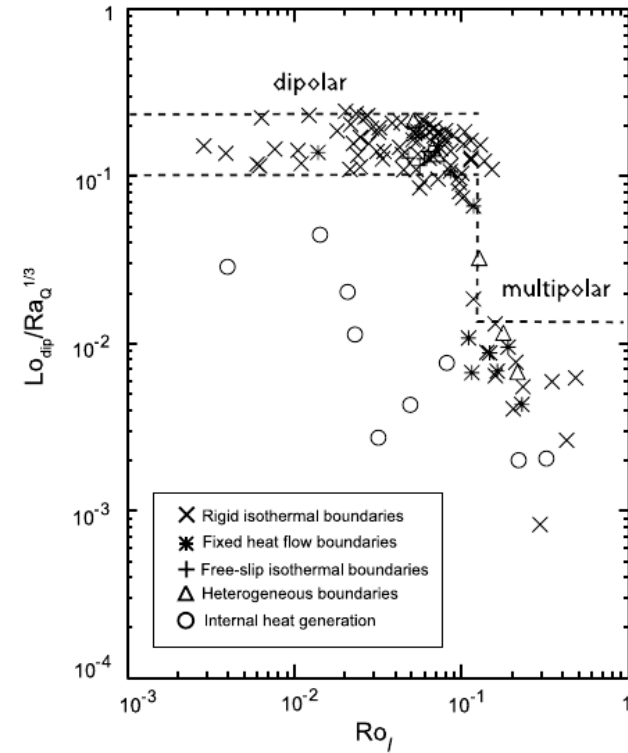
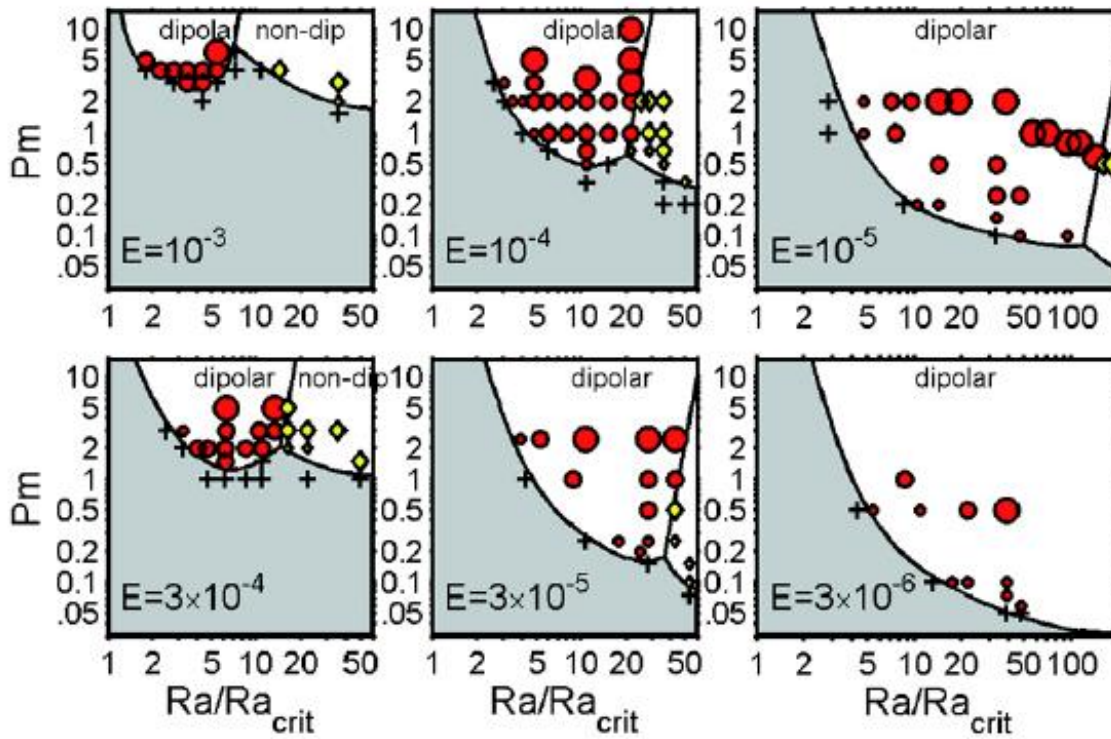
Earth-like reversals in a numerical dynamo model (Olson et al., 2009):

- High frequency dipole intensity **oscillations**.
- **Long chron**s with abrupt polarity transitions.
- Also excursions.

Problem: Often reversing dynamos not as dipolar as Earth and the non-reversing dynamos!



7. Numerical dynamos - existence of dipolar and reversing?



Systematic parametric studies show dynamo parameter dependence (Christensen and Aubert, 2006):

- Strong convection increases dynamo variability, may lead to reversals.
- Faster rotation stabilizes dipole.
- Weak Pm-dependence.

A critical local Rossby number marks a sharp transition from dipolar non-reversing to non-dipolar reversing dynamos (Olson and Christensen, 2006).

$$Ro = \frac{U}{\Omega D}$$

$$Ro_\ell = \frac{U}{\Omega L_u}$$

7. Numerical dynamos - power law extrapolations

Input parameters very far from Earth:

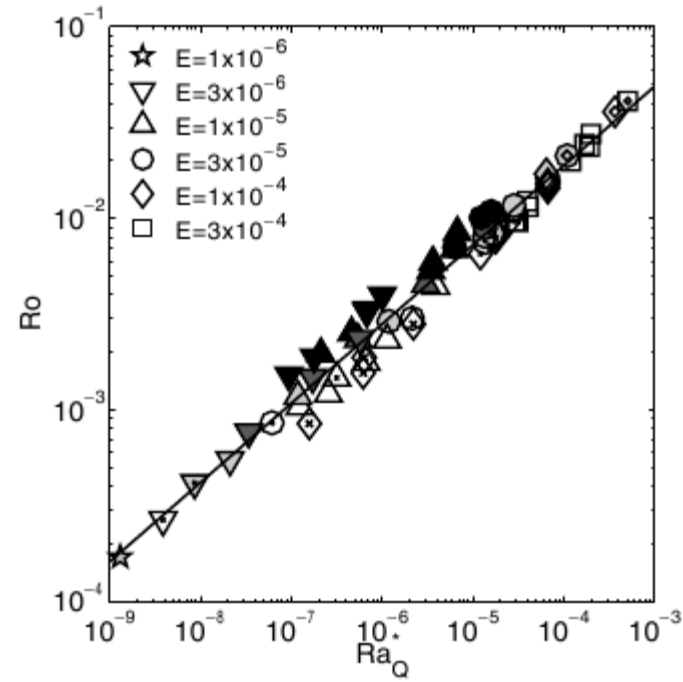
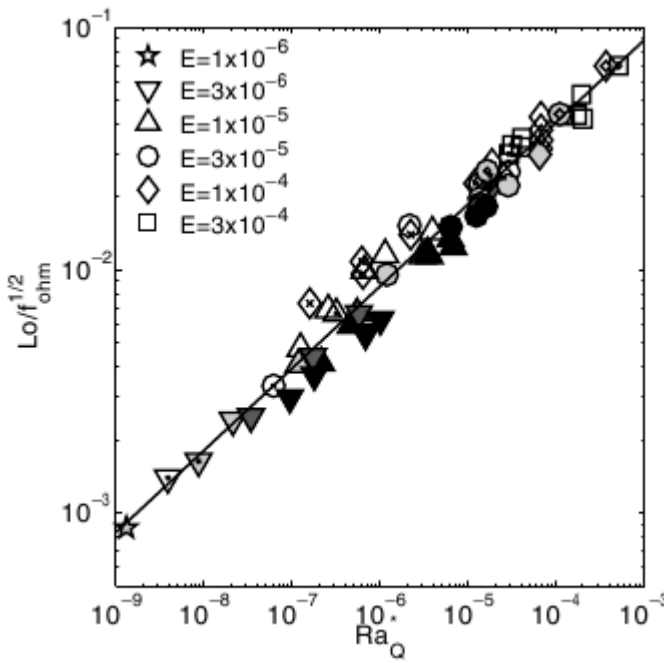
| | Dynamo models | Earth's core |
|------|-----------------------------|----------------|
| E | $1\text{e-}4 - 1\text{e-}6$ | $1\text{e-}14$ |
| Ra | $10Ra_c$ | $5000Ra_c$ |
| Pr | 1 | 1 |
| Pm | 1-10 | $1\text{e-}6$ |

Fortuitous successes? Output parameters are good!

| | Dynamo models | Earth's core |
|-----------|---------------|--------------|
| Rm | 100-1000 | 1000 |
| Λ | 1 | 1 |

Correct induction effects (correct Rm) and field strength (correct Λ). Still inferring planetary conditions from these models is debatable...

7. Numerical dynamos - power law extrapolations



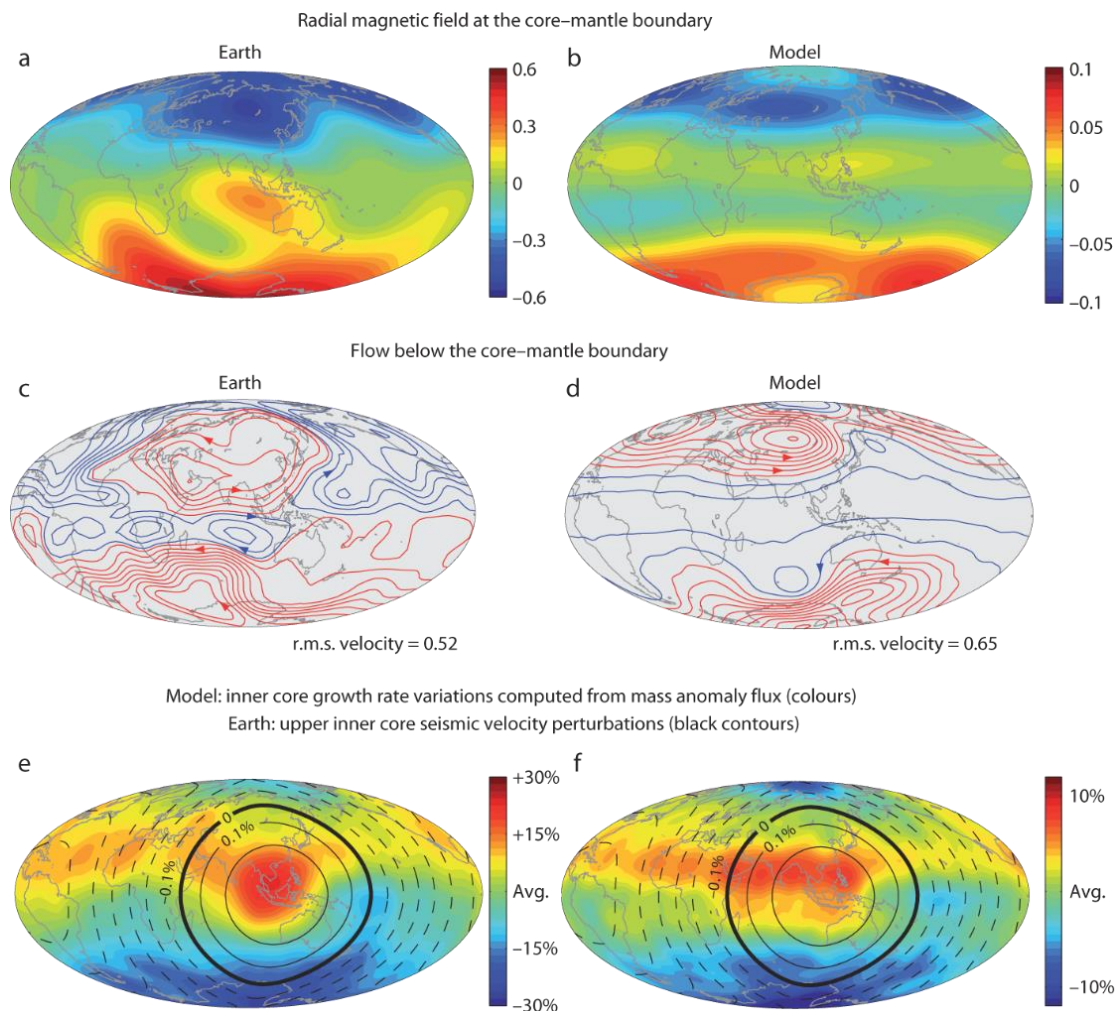
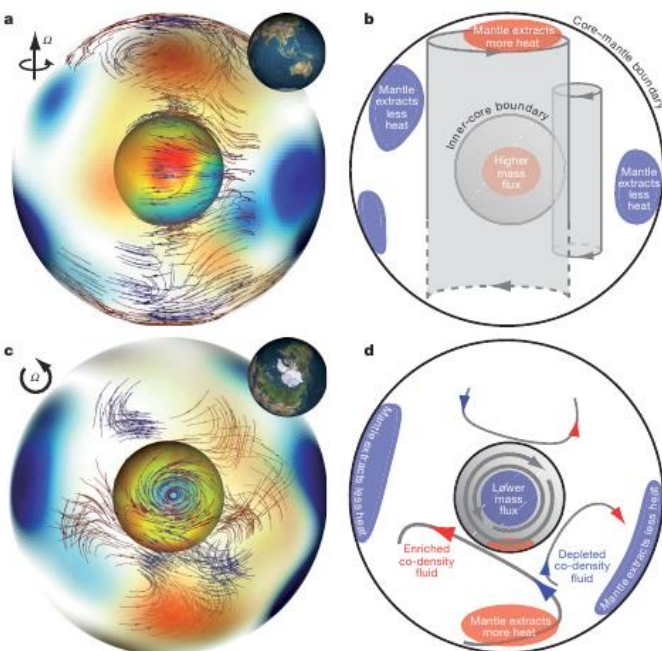
$$Ra_Q^* = \frac{1}{4\pi r_o r_i} \frac{\alpha g_o Q_{\text{adv}}}{\rho c \Omega^3 D^2}$$

Extrapolations from computationally accessible parameters to **geophysical conditions** allow inferring planetary properties (Christensen and Aubert, 2006):

- Determining property depends on the advected heat flux and **independent of (non-realistic) diffusivities**.
- Predict 1 mT field strength **inside Earth's core** (non-accessible from observations).

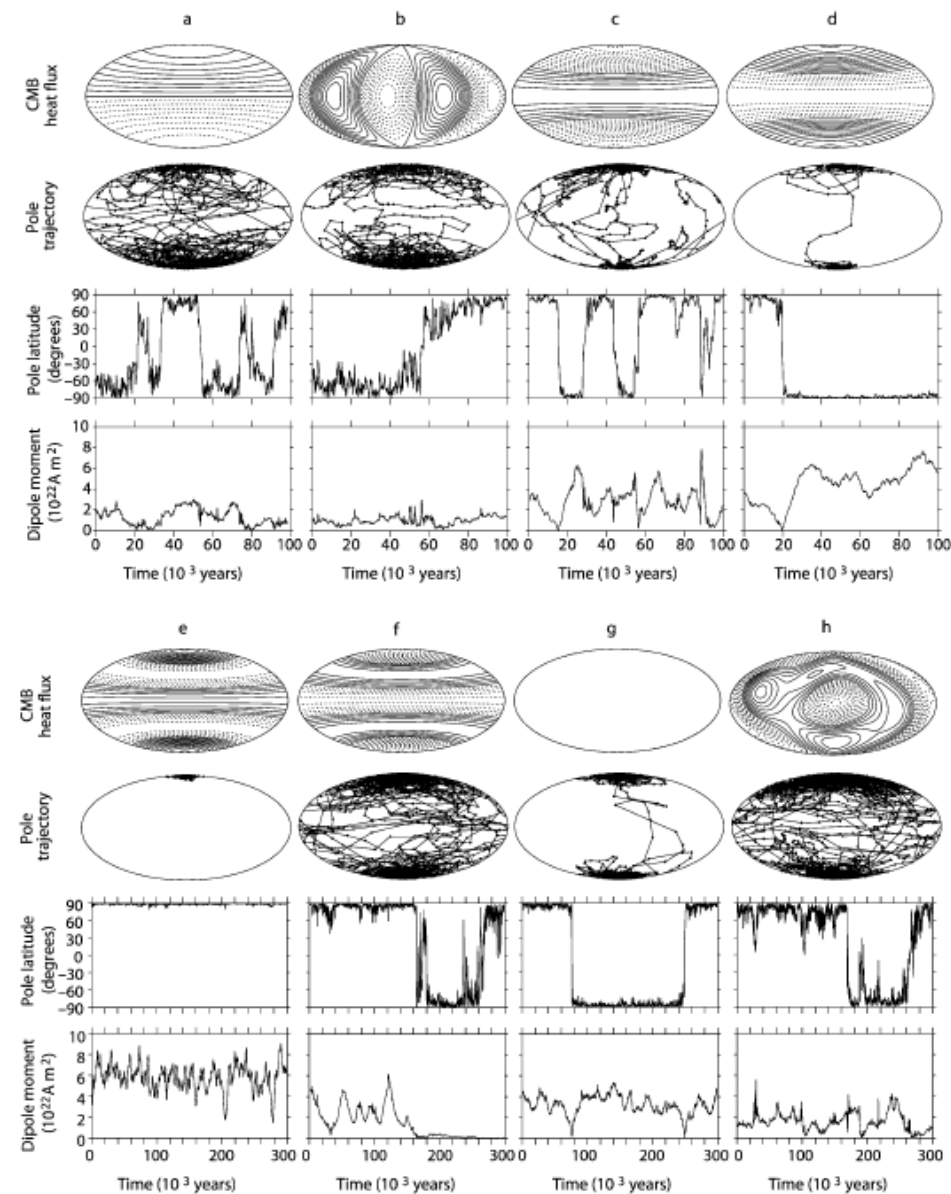
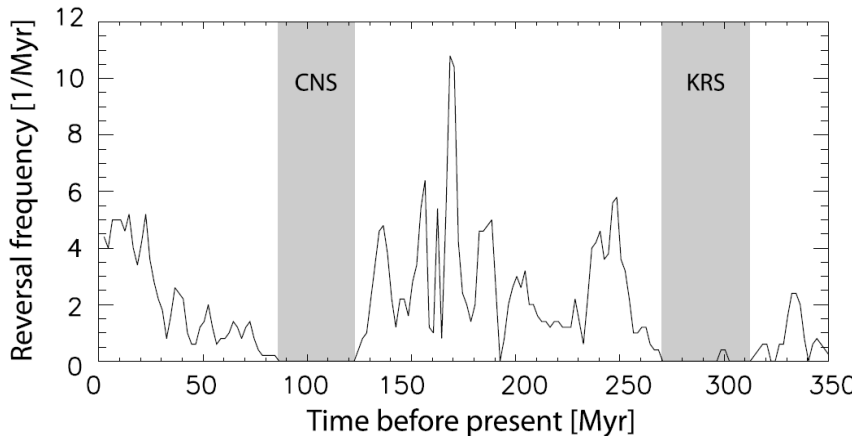
7. Numerical dynamos - mantle control explains persistent outer core observations

CMB heat flux pattern from lower mantle seismic anomalies explains patterns of time-average paleomagnetic field (past 5 Myrs), time-average inverted core flow (1840-1990) and upper inner-core seismic anomalies (Aubert et al., 2008).



7. Numerical dynamos - mantle control explains time-dependent paleomagnetic reversal frequency

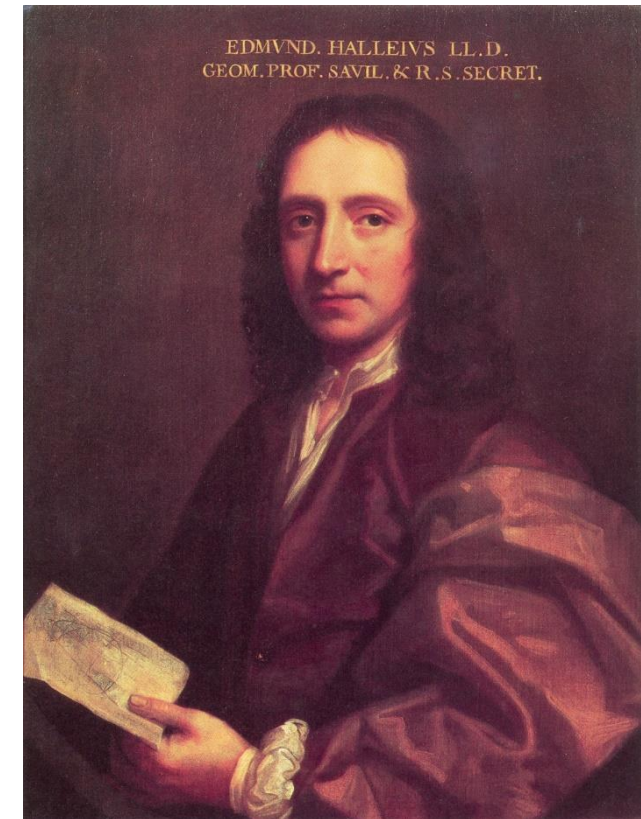
Observed changes in reversal frequency related to changes in mantle convection strength or pattern. Different imposed CMB heat flux patterns on numerical dynamos affect significantly reversal frequency, including no reversals in some cases (Glatzmaier et al., 1999).



7. Numerical dynamos - inner core control explains westward drift

An Account of the cause of the Change of the Variation of the Magnetical Needle; with an Hypothesis of the Structure of the Internal parts of the Earth : as it was proposed to the Royal Society in one of their late Meetings. By Edm. Halley.

tions, yet I found two difficulties not easie to surmount, the one was that no Magnet I had ever seen or heard of, had more than two opposite Poles ; whereas the Earth had visibly four, and perhaps more. And secondly, it was plain that those Poles were not, at least all of them, fixt in the Earth, but shifted from place to place. as appeared by the great changes in the Needles direction within this last Century of years, not only at London (where this great Discovery was first made,) but almost all over the Globe of Earth; whereas it is not known



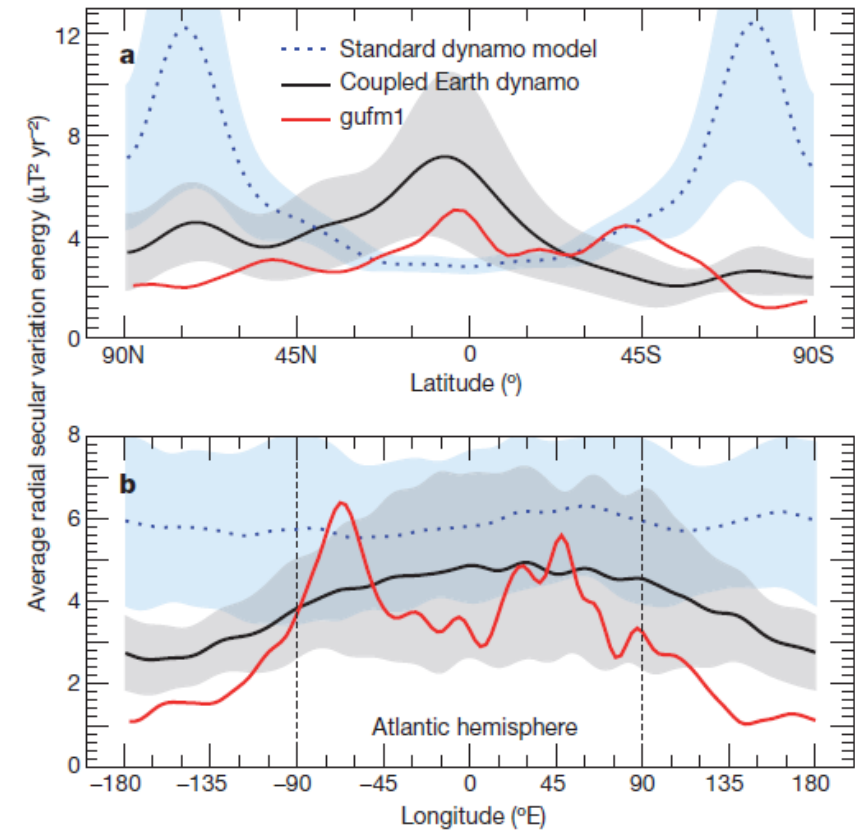
Halley (1692) discovered that the direction of the geomagnetic field varies with time. He gave examples of various locations, all show westward drift.

At Paris, Oronctius Finæus about the year 1550, did account it about 8 or 9 degrees East Variation. Anno 1640, it was found 3 degrees East. Anno 1666, there was no Variation there, and Anno 1681. I found it to be 2°. 20' to the West.

7. Numerical dynamos - inner core control explains westward drift

Aubert et al. (2013) selected a **dynamo model** that recovers observed field morphology (Christensen et al., 2010) + two additional ingredients to capture observed SV:

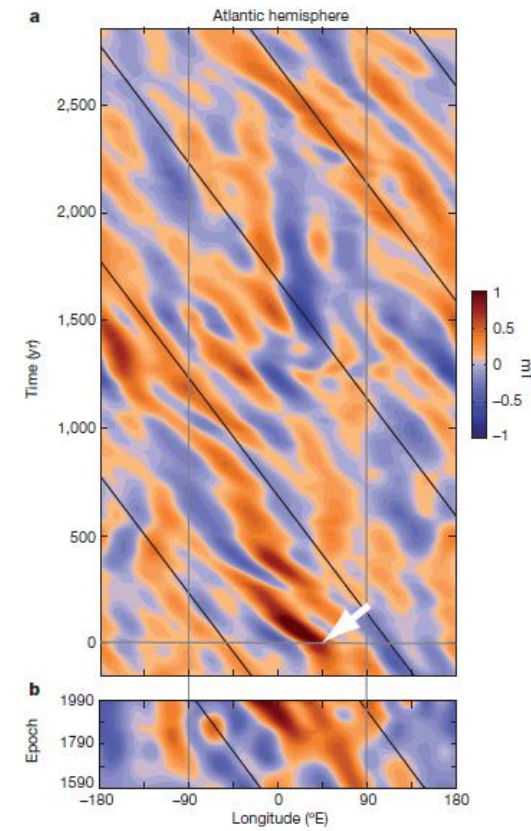
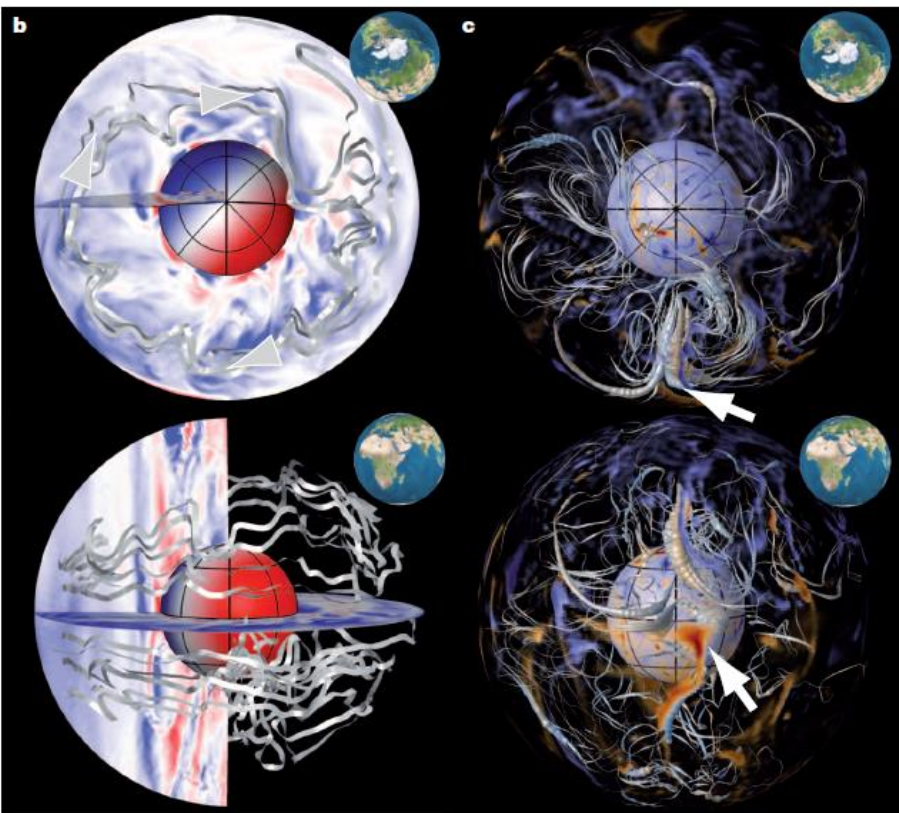
- Eastward flow at the ICB entrains the IC via magnetic IC/OC coupling. Conservation of angular momentum forces **westward drift** at the CMB via gravitational coupling between the IC and the mantle.
- Degree-1 heterogeneous ICB growth localizes the emergence and subsequent drift of the patches in the **Atlantic hemisphere** by preferential OC convection.



The dynamo model of Aubert et al. (2013) recovers strong SV at low-latitudes of **Atlantic hemisphere**.

7. Numerical dynamos - inner core control explains westward drift

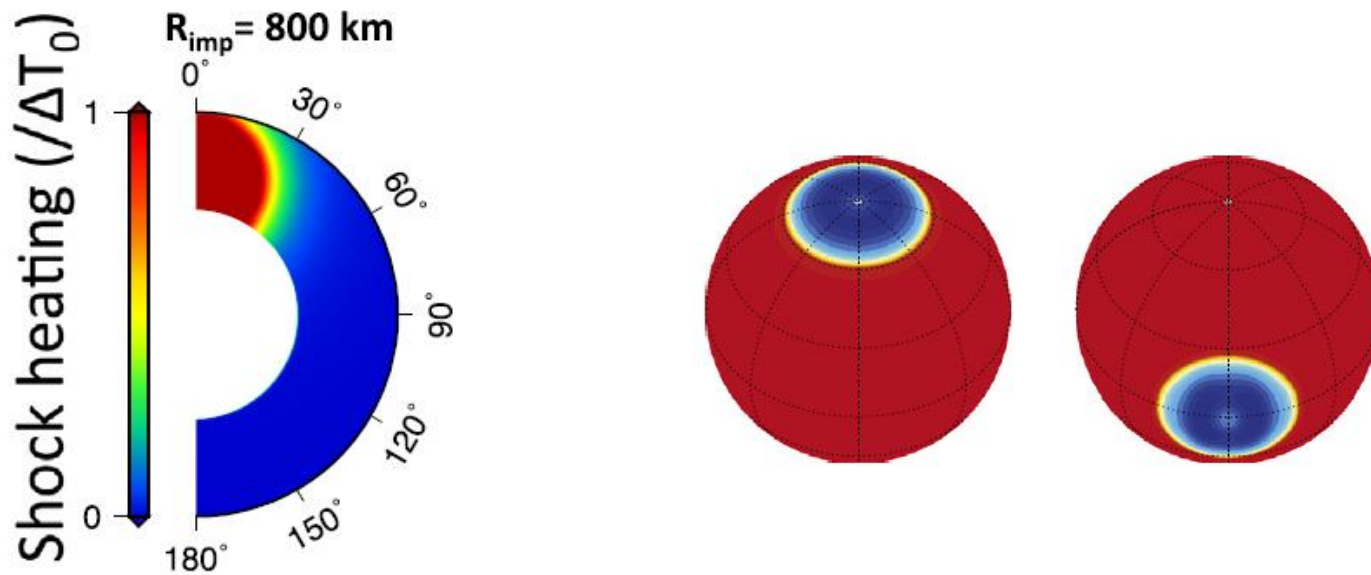
Time-longitude plot at equator shows comparable westward drift in dynamo model and Earth.



- ICB positive buoyancy flux anomaly concentrates azimuthal field lines below Indonesia (arrows) where flux is expelled to CMB.
- Westward drift carries these flux patches across Atlantic.

7. Numerical dynamos - mantle control explains Martian hemispheric field dichotomy

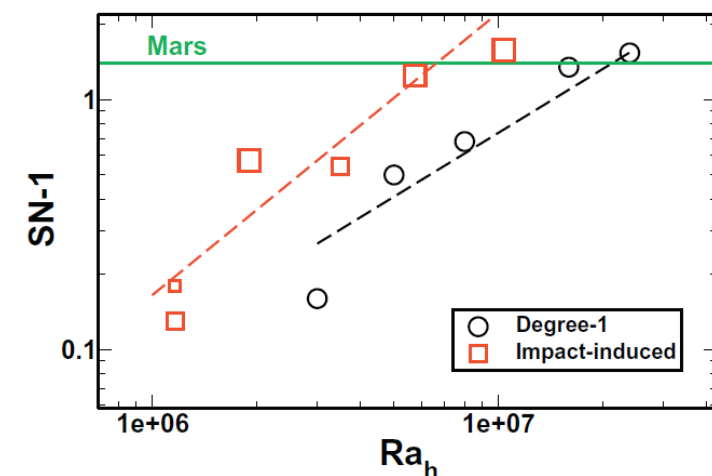
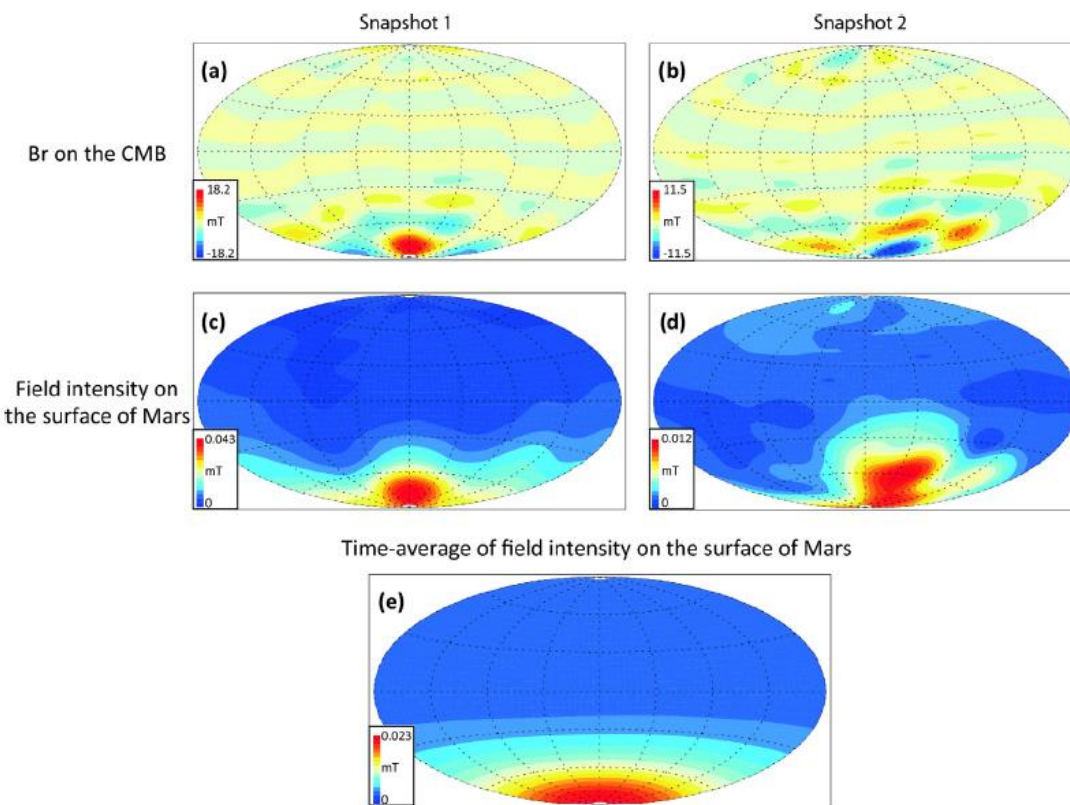
Large-scale CMB heat flux pattern explains concentration of intense magnetic crustal field in Mars' southern hemisphere as opposed to weak field in northern hemisphere (Monteux et al., 2015):



Impact-driven **shock heating** model provides CMB heat flux patterns (polar and equatorial) which are imposed as CMB heat flux on numerical dynamos.

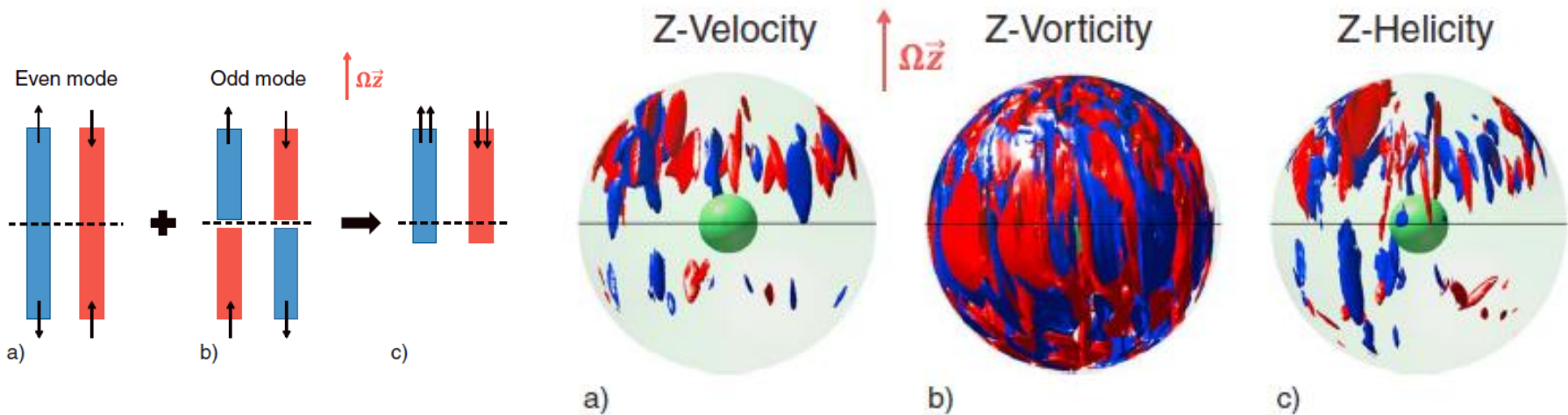
7. Numerical dynamos - mantle control explains Martian hemispheric field dichotomy

- Dynamo models with polar impactors reproduce north-south dichotomy in time-average surface field intensity.
- Impact-driven pattern more efficient than synthetic degree-1 pattern (Amit et al., 2011).
- But to reproduce Mars' amplitude of dichotomy, needs strong convection in which reversals might cause cancellations in magnetization (Dietrich and Wicht, 2013)...



7. Numerical dynamos - mantle control explains Mercury's anomalous field

Deep dynamo with **stratified layer** at the top of the core gives weak, axisymmetric and large-scale field (Christensen, 2006; Christensen and Wicht, 2008). Y20 CMB heat flux triggers non-trivial hemispherical convective instability (Cao et al., 2014):

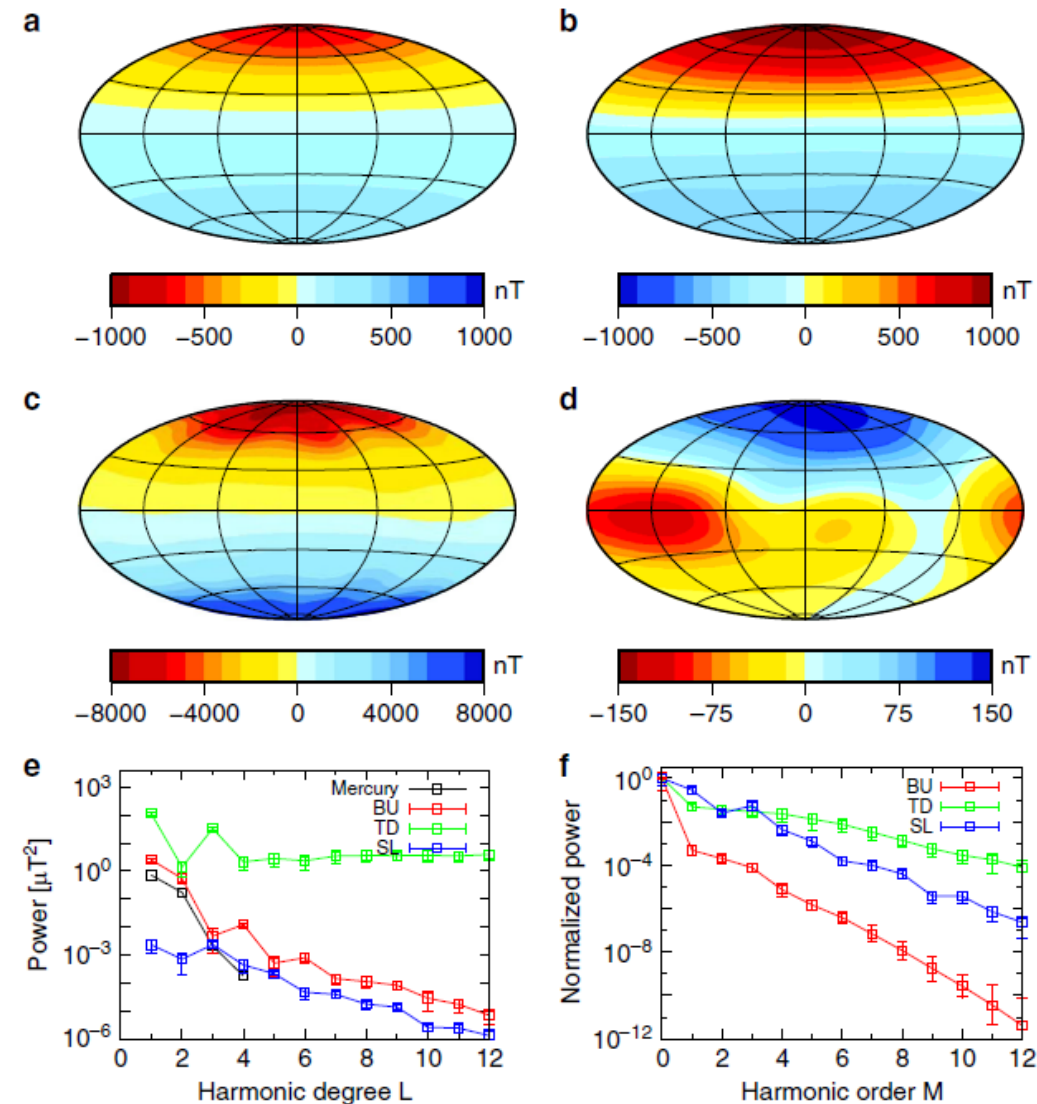


no justification for such heterogeneity at Mercury's CMB. In addition, can effects of stratification co-exist with effects of boundary heterogeneity?

7. Numerical dynamos - helicity pattern explains Mercury's anomalous field

Takahashi et al. (2019): No boundary heterogeneity, convection not hemispherical, but helicity is hemispherical!

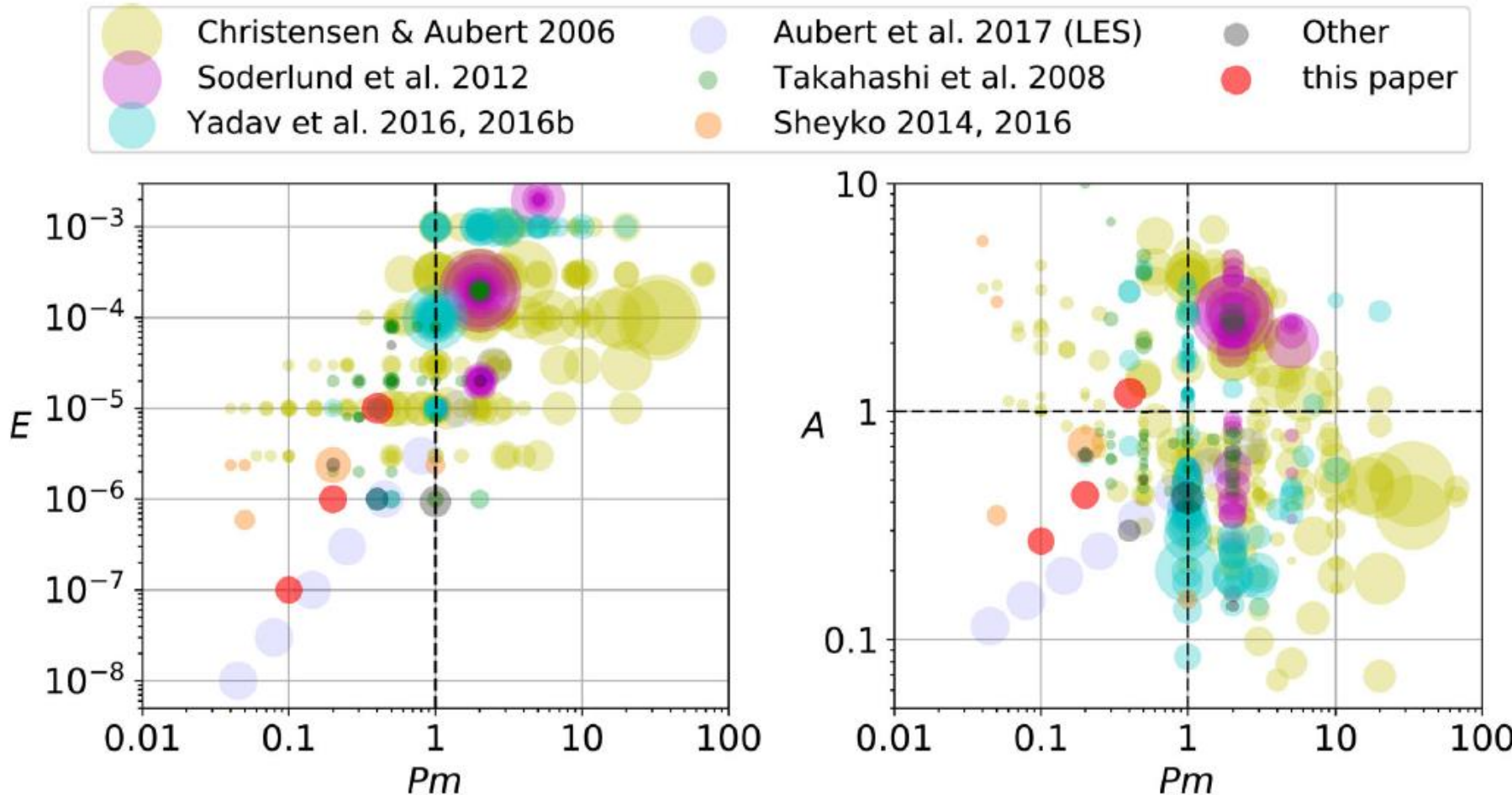
- Thermo-chemical double-diffusive convection with a stratified layer at the top of the shell.
- Magnetic force produces interaction between equatorially symmetric and anti-symmetric flows, leading to hemispherical helicity.
- Hemispherical helicity gives hemispherical field.



Bottom-up model recovers observed field.

7. Progress in numerical dynamos – exciting results!

Increasing computer power gives access to closer to Earth parameters (e.g. Schaeffer et al., 2017):

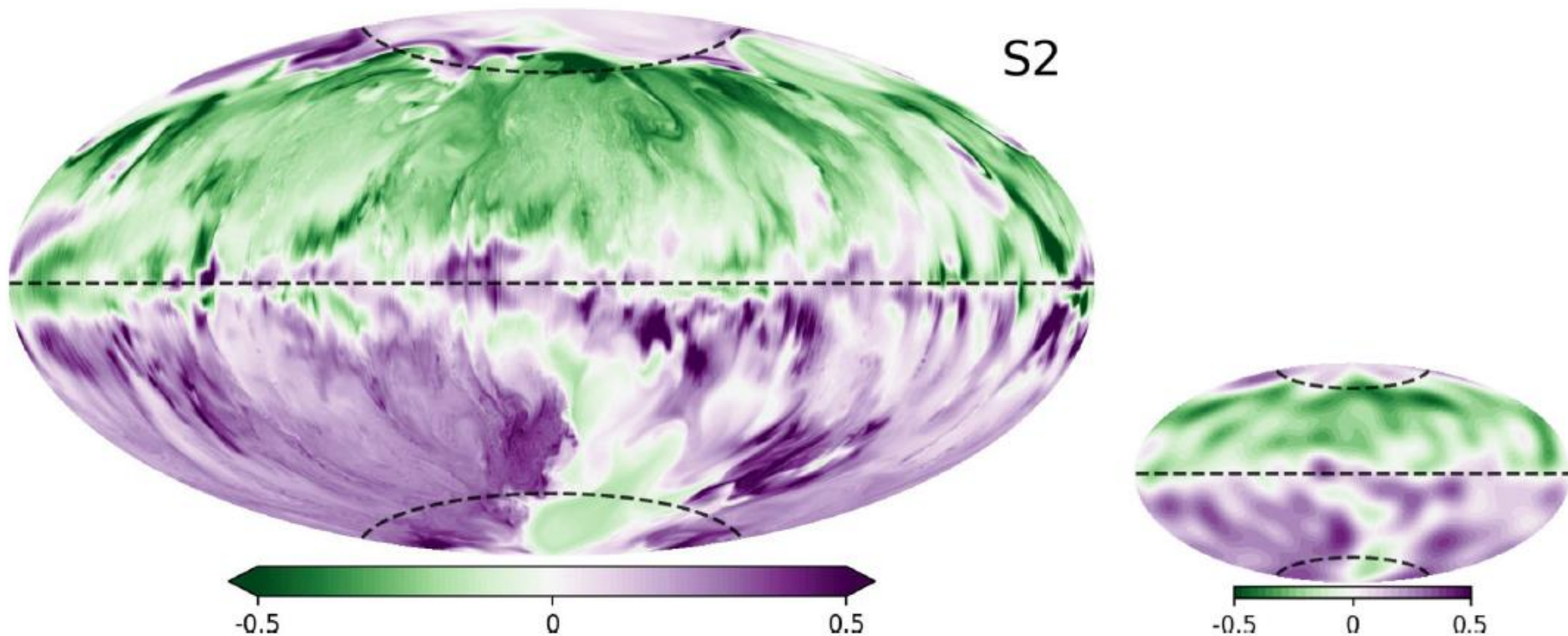


Proper modelling of turbulence, Earth-like force balance.

7. Progress in numerical dynamos - magnetic field

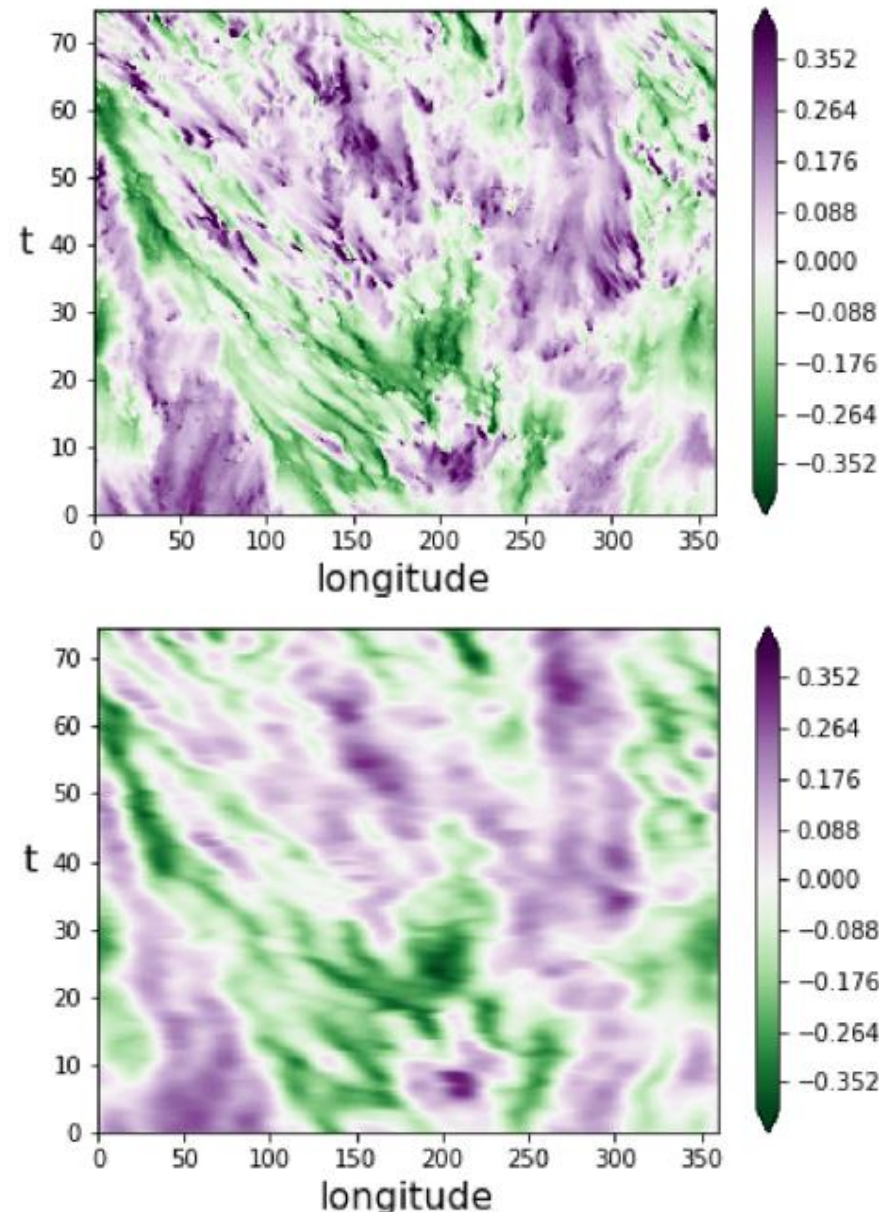
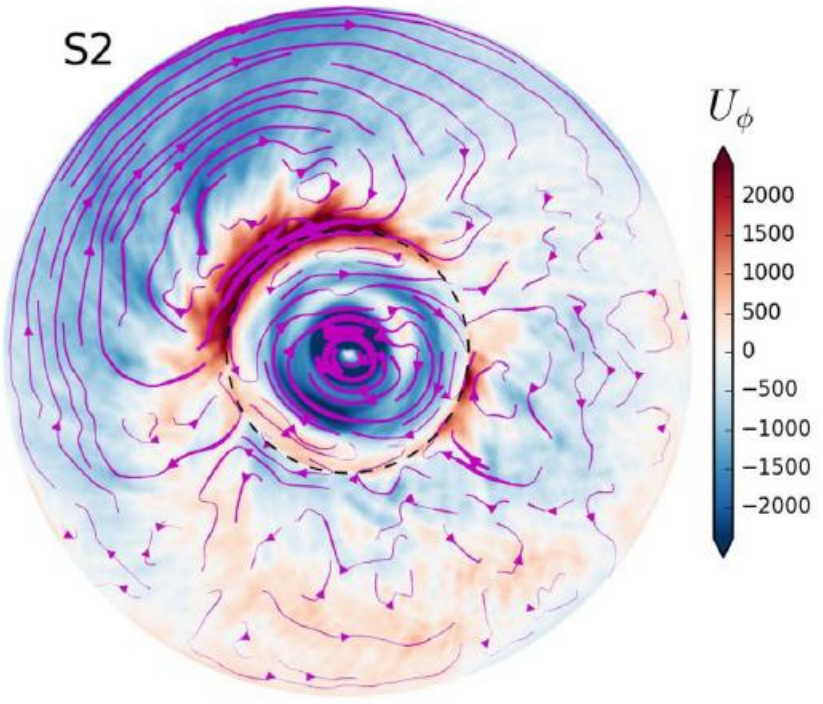
Radial field on the outer boundary (Schaeffer et al., 2017):

- Earth-like dipolarity, large-scale field.
- Reversed flux at polar regions of some snapshots.



7. Progress in numerical dynamos - gyre and westward drift

Large-scale ($m=1$) eccentric gyre (left, polar view) as in core flow inversions (e.g. Pais and Jault, 2008; Gillet et al., 2015) with low-latitudes westward drift (right, full/truncated top/bottom respectively) (Schaeffer et al., 2017), without heterogeneous boundary conditions (e.g. Aubert et al., 2013).

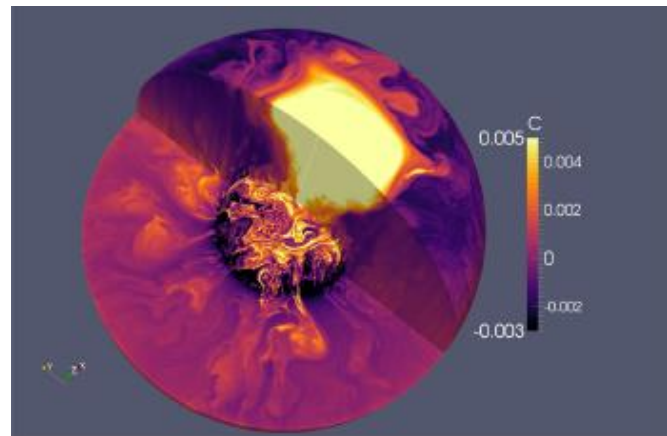


7. Recent numerical dynamos - deep dynamics

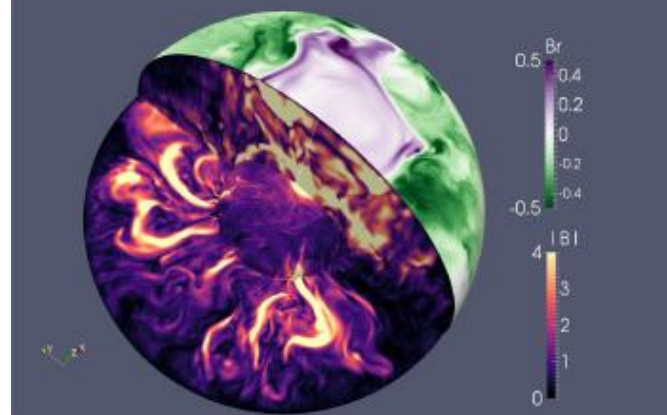
Volume images show scale separation (Schaeffer et al., 2017):

- Sharp gradients across the tangent cylinder.
- Deep field much more intense than on the outer boundary.
- Field follows co-density.

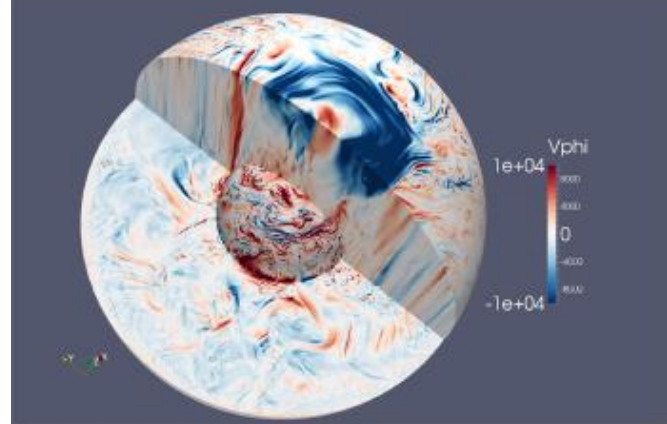
Co-density



Radial field

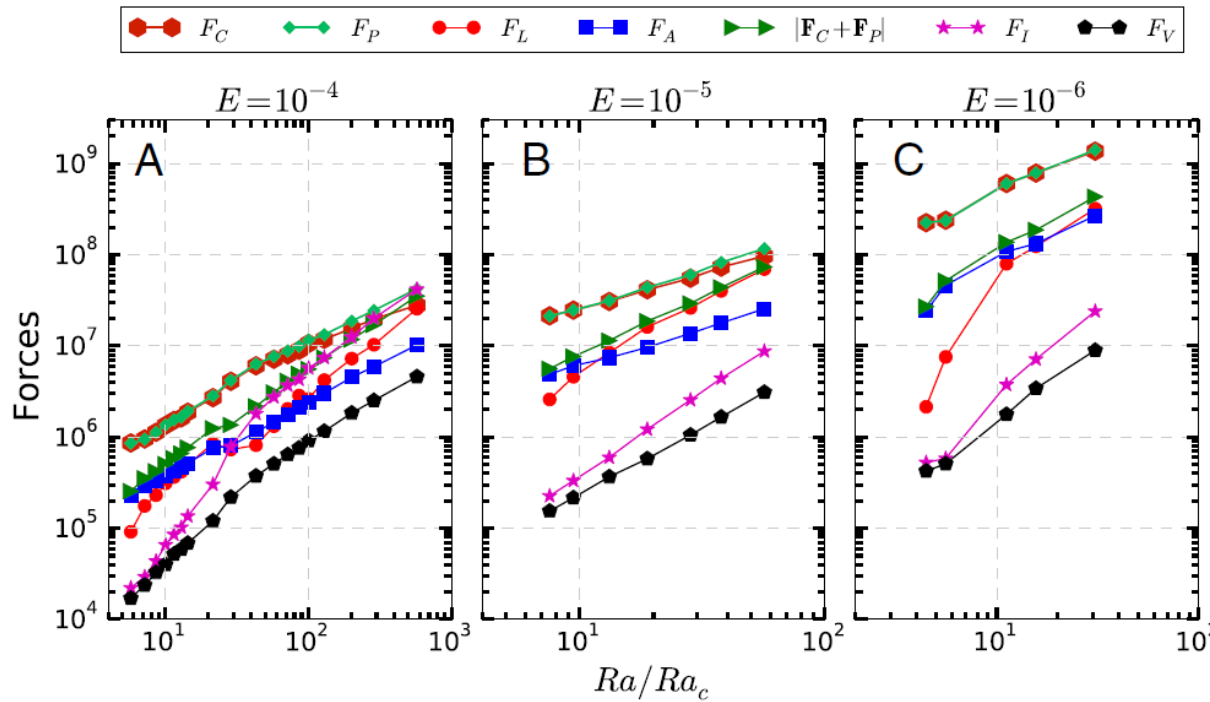


Azimuthal flow



7. Numerical dynamos - Earth-like force balance

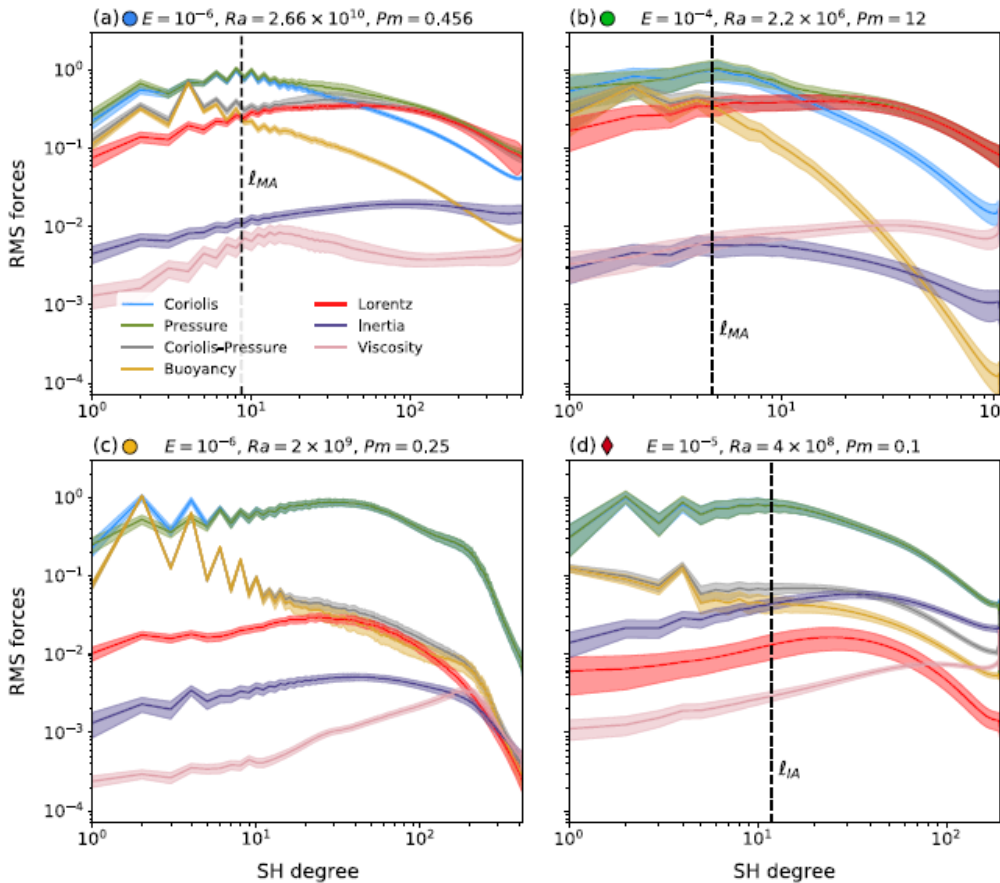
Force balance in numerical dynamos (Yadav et al., 2016):



- Zeroth order QG in agreement with theoretical expectations - very small E and Ro , small Λ_d (Soderlund, et al., 2012).
- High level of geostrophic cancellation.
- For increasing convection, first order MAC (magnetic/Archimedes/ageostrophic Coriolis) balance.
- Inertia becomes important in reversing models (only A).

7. Numerical dynamos - Earth-like force balance

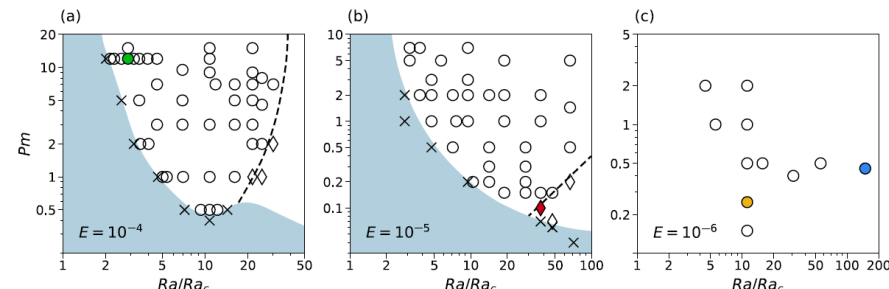
Scale-dependent force balance (Schwaiger et al., 2019):



Non-reversing QG-MAC (a, b):

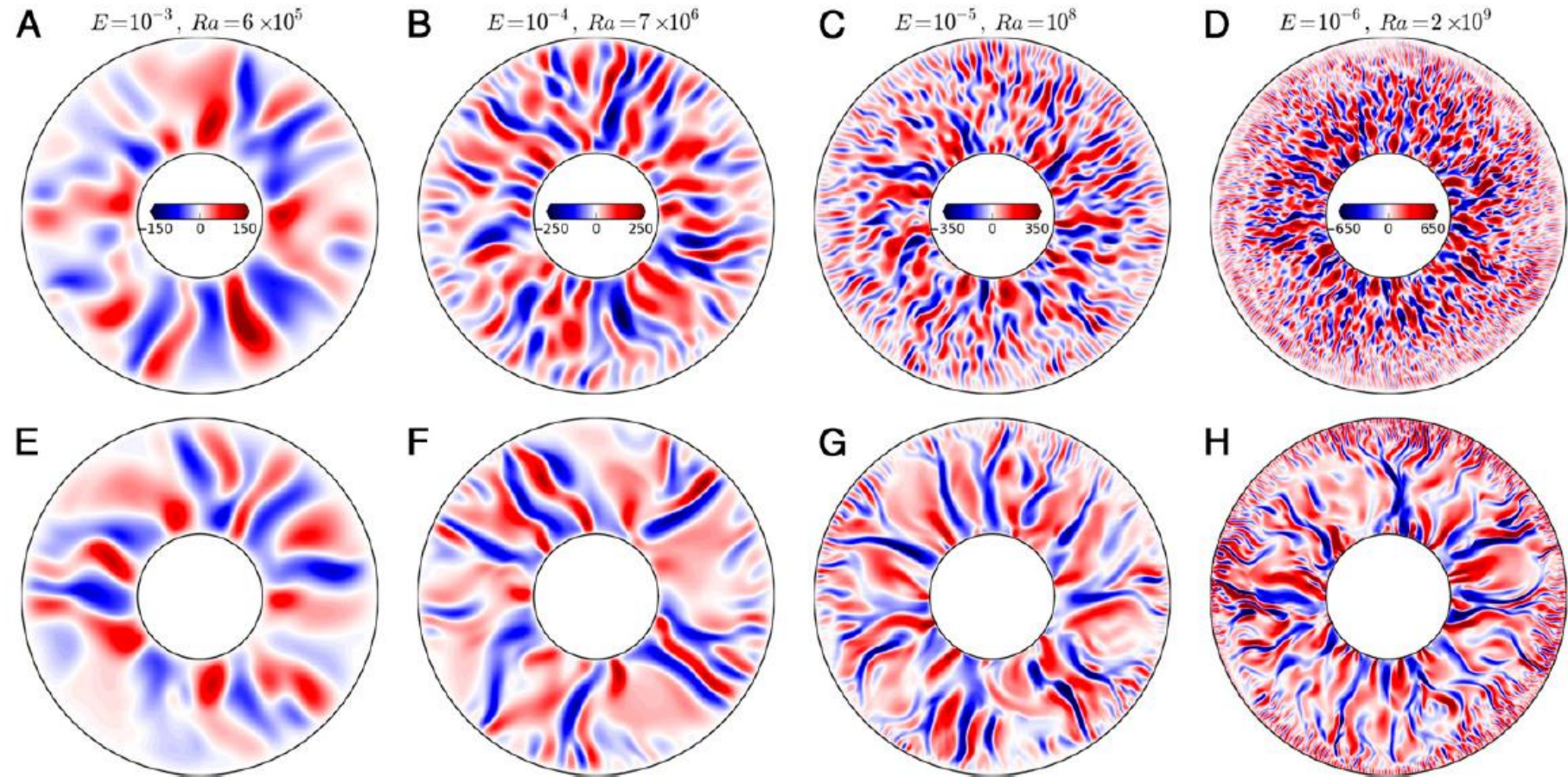
- Zeroth order QG.
- First order ageostrophic Coriolis balanced by buoyancy at large scales (thermal wind) and magnetic force at small scales.

Reversing QG-CIA (d): In multipolar dynamos first order ageostrophic Coriolis balanced by buoyancy at large scales and inertia at small scales.



7. Numerical dynamos - Earth-like force balance

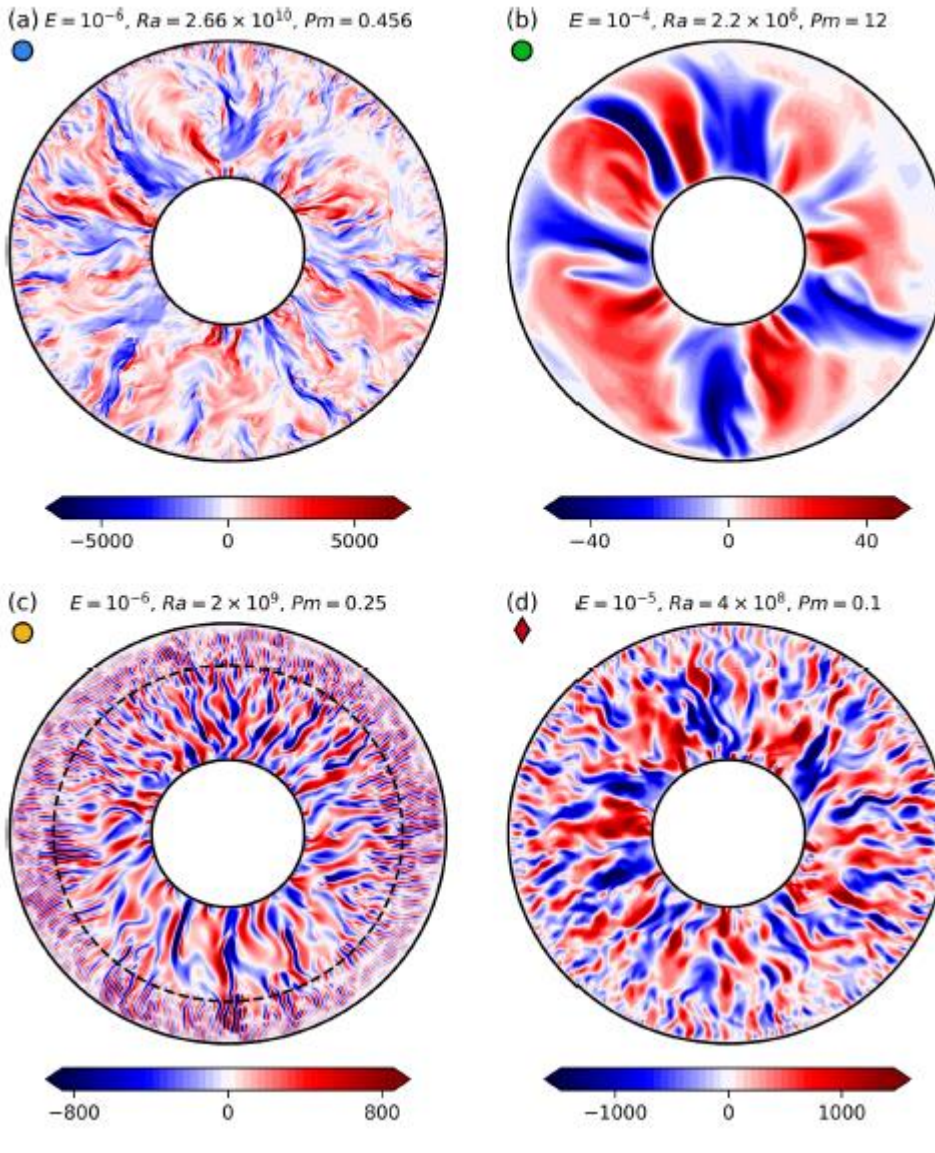
Magnetic field suppresses small-scale convection:



Radial velocity in the equatorial plane for non-magnetic (top) and dynamo (bottom) models.
From Yadav et al. (2016).

7. Numerical dynamos - Earth-like force balance

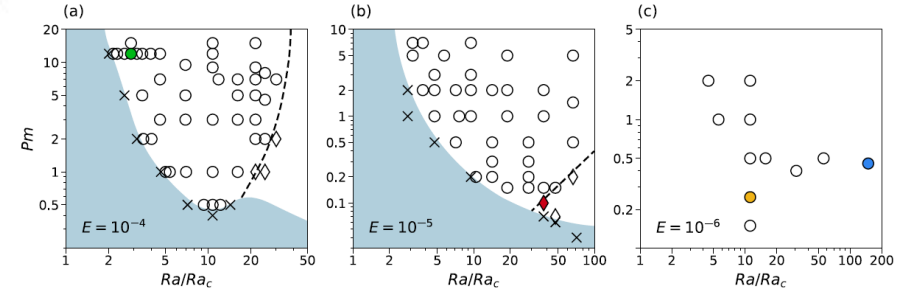
Convective pattern (Schwaiger et al., 2019):



Non-reversing QG-MAC (a, b):

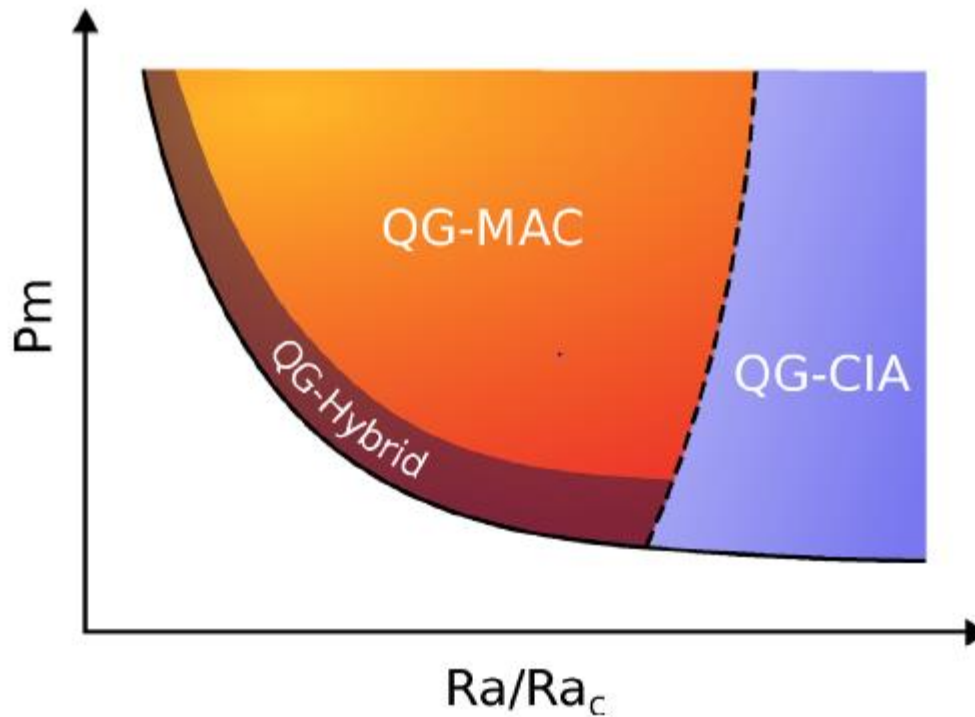
- Convective structures across the shell in both.
- Smaller scales at more super critical model (a).

Reversing QG-CIA (d): 3D small scales especially towards the outer boundary due to inertia.



7. Numerical dynamos - Earth-like force balance

Summary of dynamical regimes (Schwaiger et al., 2019):



- QG-hybrid: Near dynamo onset.
- QG-MAC: Dipole-dominated non-reversing.
- QG-CIA: Multipolar reversing.

Lower E : QG-MAC regime extended towards lower P_m and higher Ra/Ra_c .

7. Comparison between numerical dynamos and core flow inversions

| | Core flow inversions | Numerical dynamos |
|------------------|--------------------------------------|-----------------------|
| Problem | inverse, non-uniqueness | forward ✓ |
| Equations | 1 radial magnetic induction | full set of MHD ✓ |
| Self-consistent? | no | yes ✓ |
| Assumptions | many (frozen-flux, poloidal flow...) | few (Boussinesq) ✓ |
| Data? | ✓ yes | random initialization |
| Parameters | ✓ 1 realistic (infinite Rm) | Problematic? |

Use both approaches + experiments + theory...